GRANT /LANGLEY

CCMS-86-06
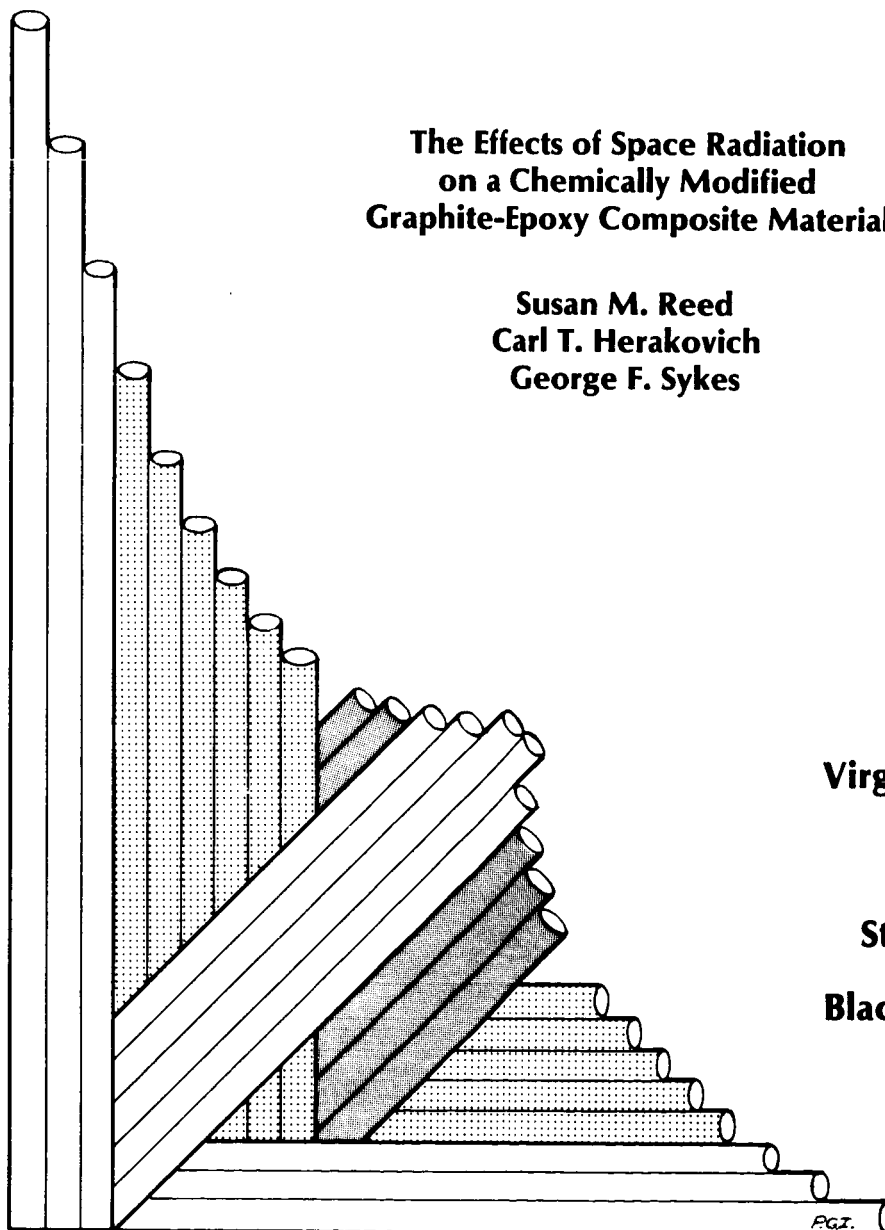VPI-E-86-19

VIRGINIA TECH

97p.

CENTER FOR COMPOSITE MATERIALS AND STRUCTURES

IN-34257

**The Effects of Space Radiation
on a Chemically Modified
Graphite-Epoxy Composite Material**

Susan M. Reed
Carl T. Herakovich
George F. Sykes

**Virginia Polytechnic
Institute
and
State University**

**Blacksburg, Virginia
24061**

College of Engineering
Virginia Polytechnic Institute and State University
Blacksburg, Virginia 24061

October 1986

CCMS-86-06
VPI-E-86-19

The Effects of Space Radiation

on a Chemically Modified

Graphite-Epoxy Composite Material

Susan M. Reed[1]
Carl T. Herakovich[2]
George F. Sykes, Jr.[3]

Department of Engineering Science & Mechanics

Prepared for:

Applied Materials Branch
National Aeronautics and Space Administration
Langley Research Center
Hampton, Virginia 23665

---

[1] Graduate Student, Department of Engineering Science & Mechanics

[2] Professor, Department of Engineering Science & Mechanics

[3] National Aeronautics and Space Administration, Langley Research Center, Hampton, VA

THE EFFECTS OF SPACE RADIATION
ON A CHEMICALLY MODIFIED
GRAPHITE-EPOXY COMPOSITE MATERIAL

(ABSTRACT)

The objective of this study was to characterize the effects of the space environment on the engineering properties and chemistry of a chemically modified T300/934 graphite-epoxy composite system. The material was subjected to 1.0×10^{10} rads of 1.0 MeV electron irradiation under vacuum to simulate 30 years in geosynchronous earth orbit.

Monotonic tension tests were performed at room temperature (75° F/24° C) and elevated temperature (250° F/121° C) on 4-ply unidirectional laminates. From these tests, in-plane engineering and strength properties (E_1, E_2, v_{12}, G_{12}, X_T, Y_T) were determined. Cyclic tests were also performed to characterize energy dissipation changes due to irradiation and elevated temperature.

Large diameter graphite fibers were tested to determine the effects of radiation on the stiffness and strength of graphite fibers. No significant changes were observed.

Dynamic-mechanical analysis demonstrated that the glass transition temperature was lowered by 50° F (28° C) after irradiation. Thermomechanical analysis showed the occurrence of volatile products generated upon heating of the irradiated material.

The chemical modification of the epoxy did not aid in producing a material which was more "radiation resistant" than the standard T300/934 graphite-epoxy system. Irradiation was found to cause crosslinking and chain scission in the polymer. The latter produced low molecular weight products which plasticize the material at elevated temperatures and cause apparent material stiffening at low stresses at room temperature.

Table of Contents

List of Illustrations

List of Tables

1.0   Introduction

1.1   Composite Materials for Space Applications

The use of advanced composite materials has increased significantly in recent years. Reasons for this increase include the distinctive characteristics of the materials. High specific strengths and stiffnesses make these materials ideal for many applications including weight critical space structures and vehicles. The high strength-to-weight and stiffness-to-weight ratios along with the flexibility of design of composite materials allow for greatly increased structural efficiency. For space vehicles, these properties mean increased range, payload, and reduced costs from fuel consumption and simplified manufacturing techniques. Because of all their advantages, composite materials are prime candidates for use in space. The NASA Large Communications Antenna and the Space Telescope (Fig. 1) are examples of high precision structures that will be placed in geosynchronous earth orbit. High stiffness truss structures constructed of graphite-epoxy composite material are currently proposed for both systems [1].
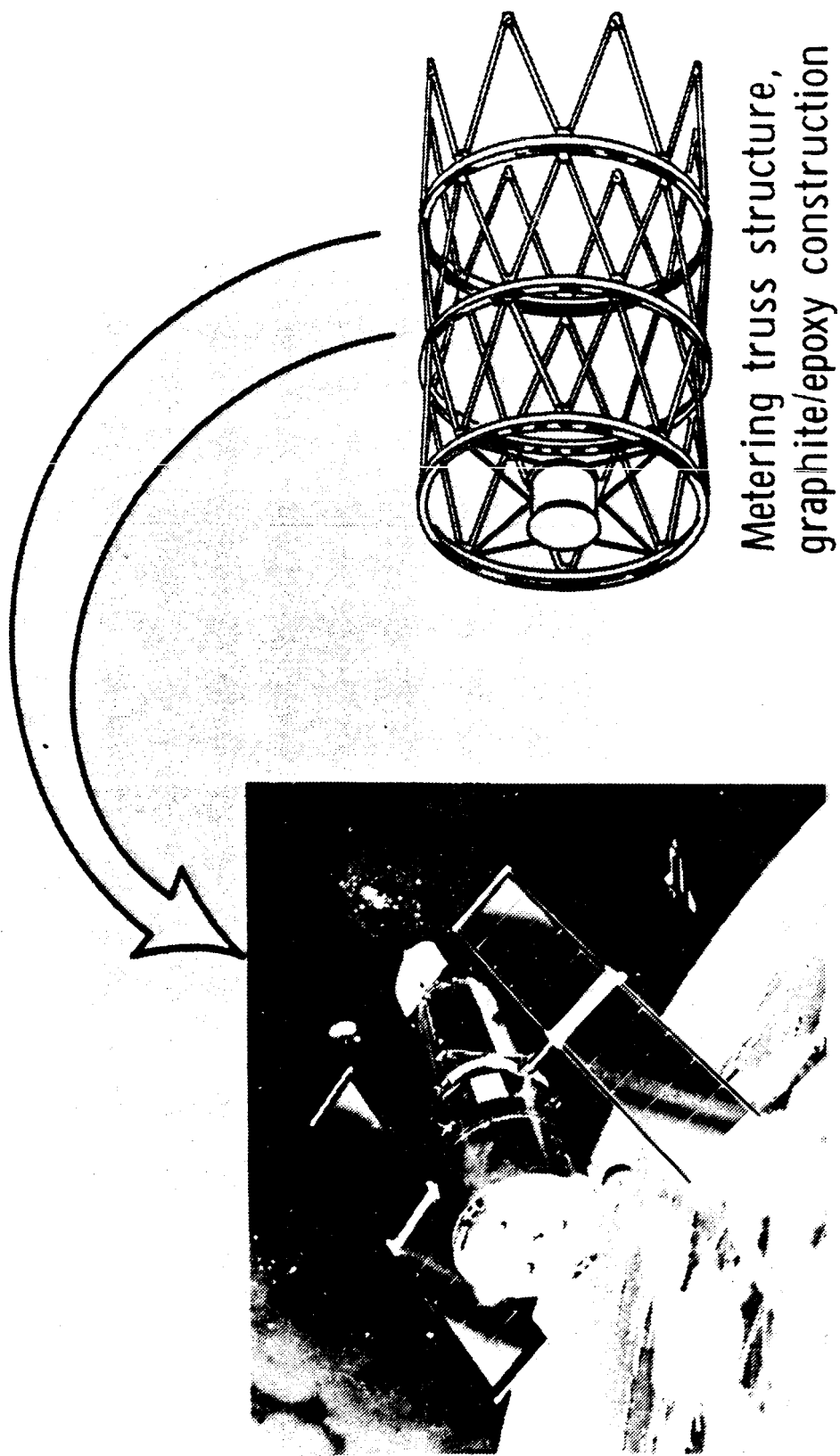
Metering truss structure,
graphite/epoxy construction

Figure 1. NASA Space Telescope and Proposed Truss Structure

The ability of composite materials to withstand the space environment will lead to their continued success and future use in space applications. However, the long-term effects of space on the behavior of these materials are still not understood thoroughly.

1.2   The GEO Environment

While in geosynchronous earth orbit (GEO), a spacecraft or structure will be in an almost perfect vacuum and subjected to temperature cycling and ultraviolet, proton and electron irradiation. Temperatures will range from the cold of space (-256° F/-160° C) to the radiant heat of the sun (248° F/120° C). This thermal cycling that a structure will experience can cause cracking, embrittlement, thermal warping, and deterioration of a structure's surface. The vacuum environment can cause vacuum outgassing, which is a loss of solvents and moisture that results in dimensional and mechanical property changes. Ultraviolet irradiation is an electromagnetic radiation produced by the sun. It only affects the surface of a structure. Proton and electron irradiation are present from trapped particles, such as those that occur in the earth's Van Allen radiation belt. The proton irradiation, like the ultraviolet irradiation, only affects a structure's surface, but the electron irradiation can be highly penetrating. Long-term exposures, such as ten to thirty years in geosynchronous earth orbit, will lead to electron radiation dosage levels of 10^9 to 10^{10} rads. Furthermore, the electron radiation effects of the space environment not only depend upon the radiation exposure, but also on the other environmental parameters of temperature and high vacuum.

1.3 Objective of the Present Study

This research will attempt to further the understanding of the interaction of some environmental conditions of space on graphite-epoxy composite material. Previous work performed by Milkovich, Herakovich and Sykes, [2] characterized the effects of electron radiation, vacuum and temperature on the engineering properties, dimensional stability and chemistry of a graphite-epoxy fiber-reinforced composite material. The material was the T300/934 system of Thornel (Union Carbide) T300 fibers in a Fiberite 934 epoxy resin. Milkovich et al. found that the epoxy matrix is degraded by electron radiation in a manner which is influenced significantly by temperature. In general, in-plane elastic and strength properties of the composite were degraded by exposure to electron radiation. They concluded that the degradation is due to low molecular weight products generated mainly from the epoxy's processing additives during irradiation and recommended that these additives be removed from the composite system in an attempt to create a more radiation resistant epoxy.

The objective of the present study is to examine the mechanical behavior of a modified T300/934 graphite-epoxy. The modification consisted of removing those additives thought to be the cause of the degradation observed in the previous study. Additionally, this study will investigate the unloading response of irradiated graphite-epoxy and the influence of electron radiation on graphite fibers.

2.0 Procedure

2.1 Materials

2.1.1 Modified Graphite-Epoxy

The graphite-epoxy composite material used for the initial work by Milkovich et al. [2] was a T300/934 system. For the current work, in the attempt to make the material more radiation resistant, the Fiberite 934 epoxy resin was modified. The low molecular weight by-products that caused delamination of the irradiated standard material were believed to come from the epoxy processing additives [3]. Therefore, the main processing additive was not included in the epoxy used to fabricate the present panels.

The chemistry of the 934 epoxy is shown in Fig. 2. The processing additive of diglycidyl orthophthalate (GLYCEL-100) was removed to form the modified epoxy. Samples of the graphite-epoxy panels made with this modified epoxy were tested for fiber volume fraction, volatile content and density. This data, along with the standard material data, are presented in Table 1.
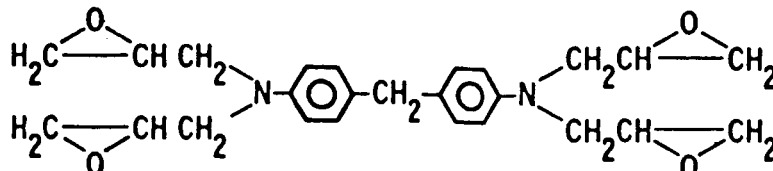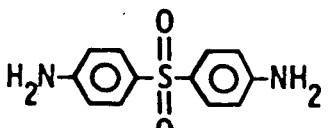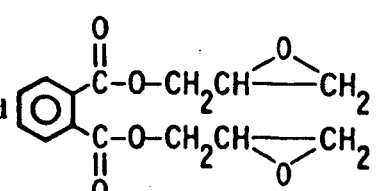
Tetraglycidylmethylenedianiline (MY-720)   64

Diaminodiphenylsulfone (DDS)   25

This processing
additive removed
to modify the
epoxy.

Diglycidyl orthophthalate (GLYCEL-100)   11

$F_3B \cdot NH_2-CH_2-CH_3$

Boron Trifluoride-
monoethylamine complex (BF_3) 0.4

Figure 2.   Chemical Modification of the Fiberite 934 Epoxy Resin

Procedure

6

Table 1. Material Properties for Standard and Modified T300/934 Graphite-Epoxy

T300/934 GRAPHITE-EPOXY		
	Standard Material	Modified Material
Fiber Volume Fraction	68%	61.5 - 64%
Volatile Content	< 1%	< 0.6%
Density	1.568 g/cm³	1.54 g/cm³

Coupon Specimens

Coupons, of the dimensions given in Fig. 3 and shown in Fig. 4, were cut from eight unidirectional, 4-ply panels, which were made by the Hexcel Corporation in California. As noted by Haskins [4], and especially because this material was a one-of-a-kind, coupons for each orientation were cut from the the same panel. Two of these panels were C-scanned to insure integrity. The irradiated coupons were exposed to 1.0 MeV electrons for a total dosage of 1×10^{10} rads to simulate a "worst case" of 30 years in space. Electrons with 1.0 MeV energies are characteristic of those found in the earth's Van Allen belt. The radiation was achieved at a rate of 5×10^7 rads per hour for 200 hours (this correlates to nine to ten days of use time at the radiation facility described below).

All coupons, both baseline (non-irradiated) and irradiated, were strain gaged with high temperature gages and lead wires at NASA Langley Research Center (LaRC). The $[0]_4$ specimens were fitted with two single gages, one parallel and one perpendicular to the fiber direction. From these tests, the in-plane mechanical properties determined were Young's modulus, E_1, Poisson's ratio, v_{12}, and the longitudinal tensile strength, X_T. The $[90]_4$ specimens had a single gage aligned along the longitudinal axis. From these specimens, the transverse modulus, E_2, and the transverse strength, Y_T, were determined. The $[10]_4$ and $[45]_4$ off-axis specimens had rectangular rosette strain gages to measure strains 0°, 45°, and 90° from the longitudinal axis. The shear modulus, G_{12}, was determined from the off-axis coupons using the formulation in Appendix A.1. The test matrix for the monotonically loaded specimens is included in Table 2.

Any misalignment of the strain gages with respect to the specimen principal axis was determined with a Photoelastic Inc. Polaris magnifier. The strain gage area was magnified 10X and projected to the viewing screen. The misalignment angle was measured from the screen with the aid of crosshairs. Calculations for true strains from the strains measured are found in Appendix A.2.

Modified T300/934 graphite-epoxy

6 in. (15.24 cm)

Fiberglass
tabs

Wide temperature range
strain gages

1 in.
(2.54 cm)

1/2 in.
(1.27 cm)

4-plies thick
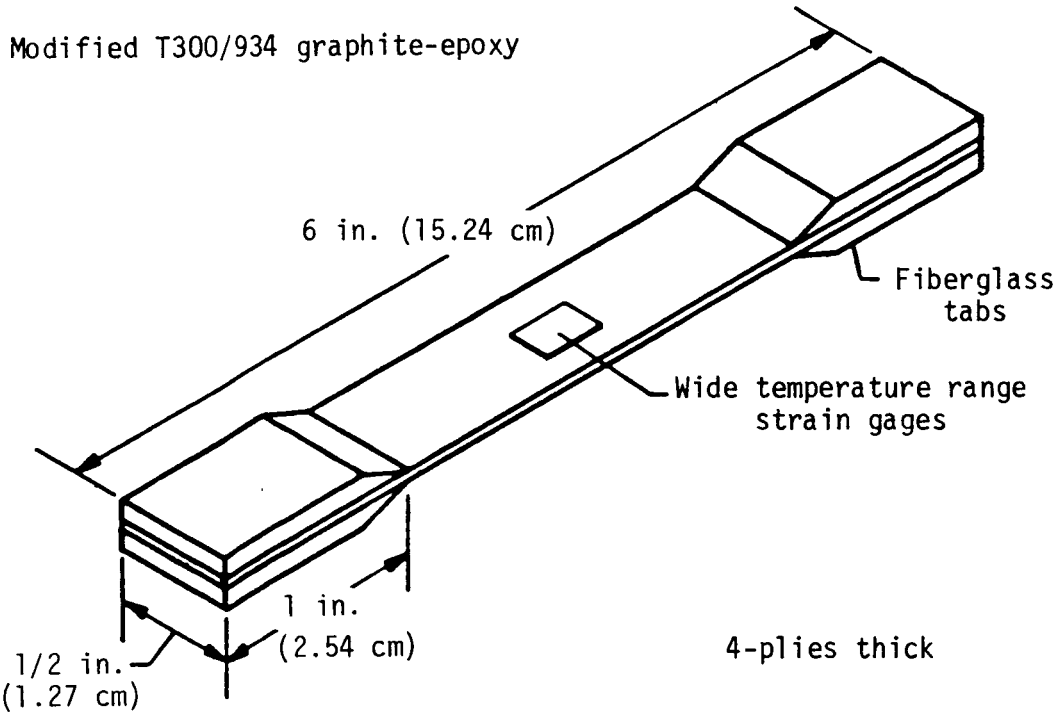
Figure 3. Tension Test Coupon Schematic
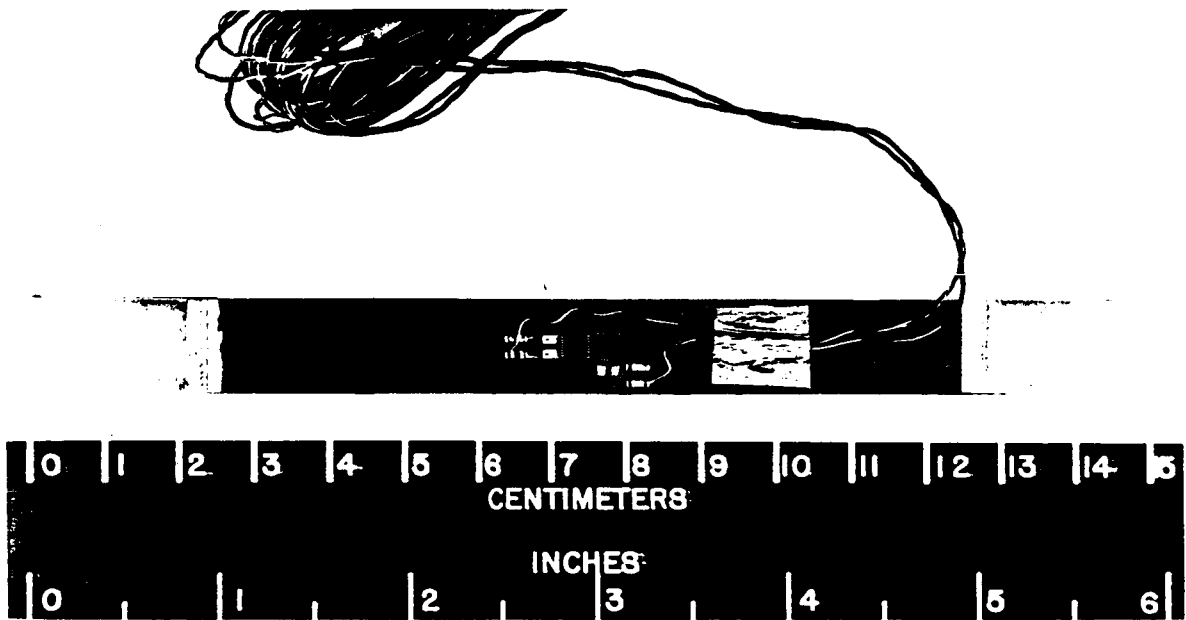
Figure 4. Tension Test Coupon

Table 2
Test Matrix

T300/934 GRAPHITE-EPOXY

Specimen	STANDARD MATERIAL				MODIFIED MATERIAL							
	Cyclic Loading				Monotonic Loading				Cyclic Loading			
	Baseline		Irradiated		Baseline		Irradiated		Baseline		Irradiated	
	RT	ET	RT	ET	RT	ET	RT	ET	RT	ET	RT	ET
[0]$_4$	0	0	0	0	5	4	3	4	0	0	0	0
[10]$_4$	3	3	3	3	3	3	3	3	3	3	3	3
[45]$_4$	3	3	3	3	7	4	4	3	5	5	3	5
[90]$_4$	0	3	0	3	3	3	3	3	0	3	0	3

RT: Room Temperature (75°F/24°C)
ET: Elevated Temperature (250°F/121°C)

It was necessary to bond fiberglass tabs to the ends of these thin coupons for load introduction. The tabs also prevent damage from the mechanical grips biting into the specimen during loading. Dexter Hysol type 934NA room temperature curing epoxy mixed with 5 micron glass beads was used to adhere the tabs to the sandblasted ends of the specimens.

After the specimens were irradiated, strain gaged and tabbed, they were dried in an oven. This was done to eliminate any effects that moisture might have on the mechanical properties and to insure that all specimens were tested with the same moisture content. A sample piece of material was dried with the specimens and its weight was monitored until no further weight loss was recorded. The total amount of moisture removed from the sample corresponded to 1% of its original weight. This procedure took approximately two weeks in a vacuum chamber with no heat added. It also took approximately two weeks in a standard oven at 110° F with no vacuum. The latter was used at Virginia Tech, while the former was used at LaRC.

Rotating mechanical grips were used to allow the introduction of a sufficiently homogeneous stress field at the location of the strain gages and to reduce the stress concentrations in the grip region as much as possible. The reduction of stress concentrations helped obtain higher ultimate loads which were more representative of "true" material strength properties of the monotonically loaded specimens [5]. Much care was taken in the alignment of the coupons in the test grips (Fig. 5). Also, a support arm was used to brace the coupon while mounting the test fixture into the testing machine (Fig. 6).

2.1.3 Fiber Specimens

Single, non-sized, graphite sheath and core fibers (not tows) from Hough Laboratories in Springfield, Ohio were tested in tension in order to investigate the previously used assumption that graphite fibers are inert to radiation. The fibers were cut and randomly divided for two groups:
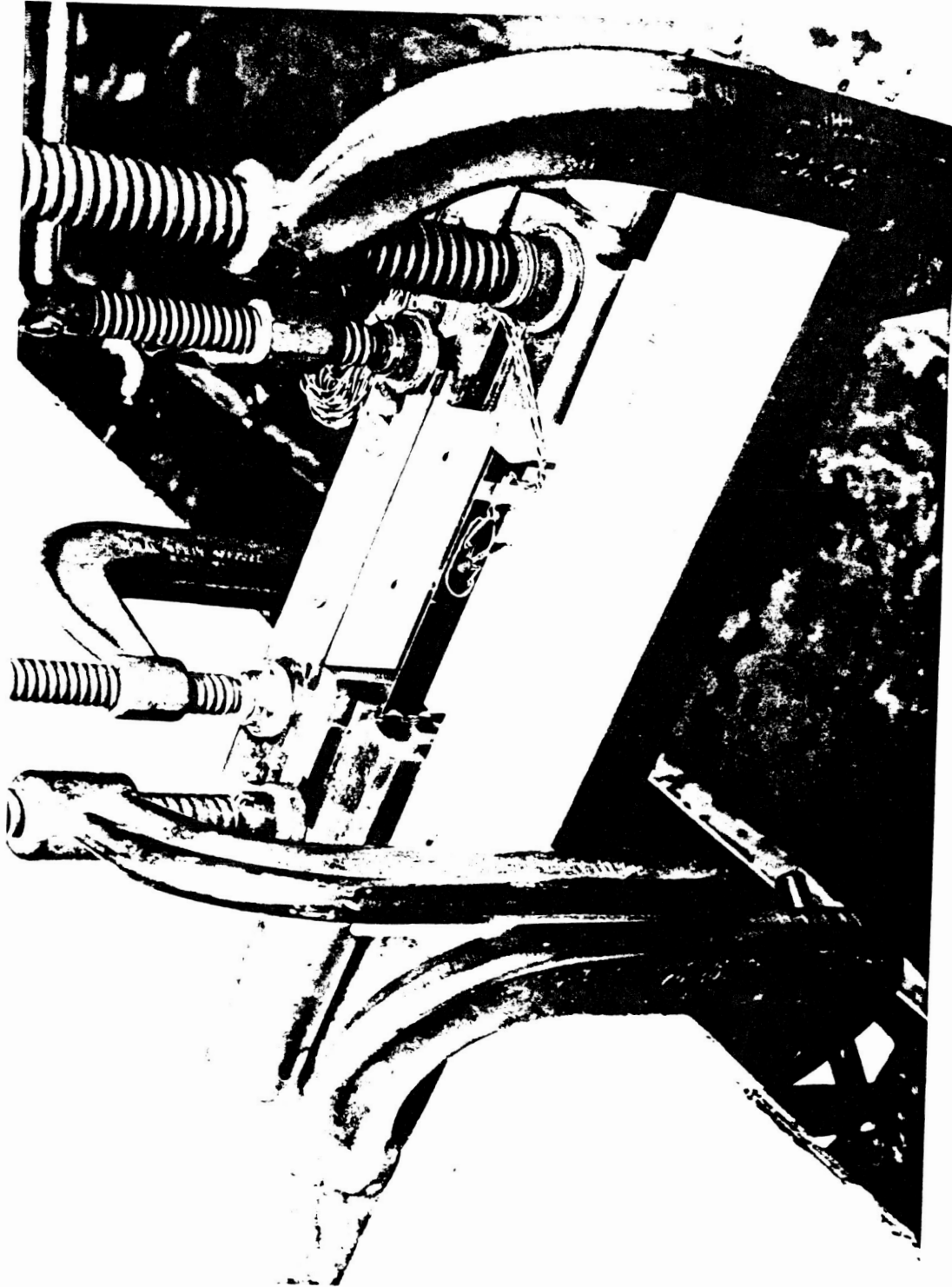
Figure 5. Coupon Mounted in Tension Test Grips with Alignment Bar
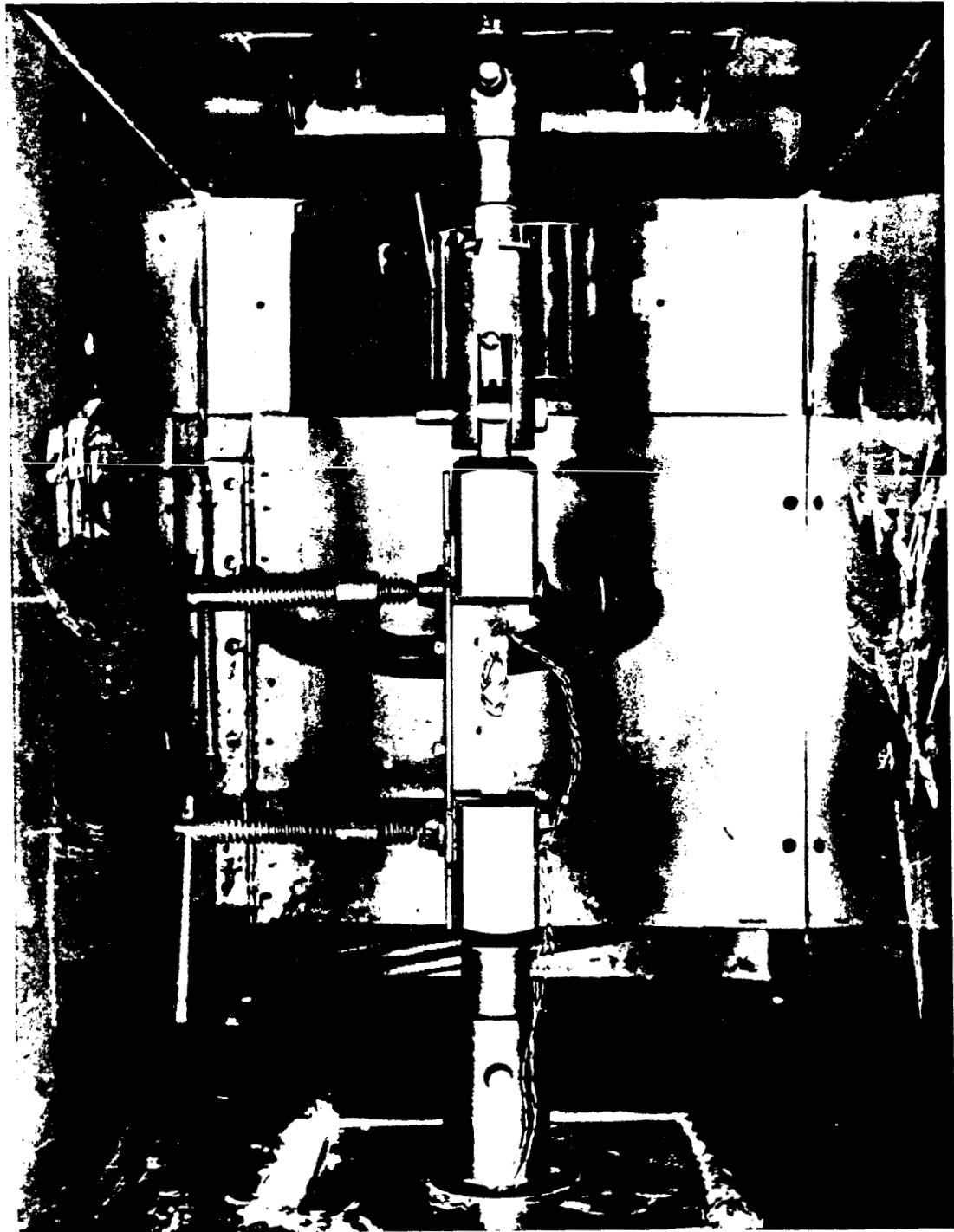
Figure 6.   Test Fixture in Instron Test Chamber

baseline and 1.0×10^{10} rads. The baseline and irradiated fibers were mounted in cardboard tabs using the same epoxy used to adhere the fiberglass tabs to the coupons. The tabbed fibers were then placed in moment free grips (Fig. 7) used for testing film samples on the 10 lb. (4.5 kg.) Instron machine. A 2″ (51 mm) gage section was used for these nominally 0.0033″ (0.084 mm) diameter fibers.

2.2   Testing Facilities and Equipment

The experiments for this study were conducted partly at NASA Langley Research Center in Hampton, VA and partly at Virginia Polytechnic Institute and State University in Blacksburg, VA. For coupon tensile testing the same basic experimental procedure was used, although equipment varied slightly.

2.2.1   Specimen Irradiation

All irradiation of coupons and fibers was performed at NASA Langley Research Center's Space Materials Durability Laboratory. This facility uses an electron accelerator, which, in a 10″ (254 mm) diameter beam, can produce exposures of the magnitude required. The composite samples to be irradiated are flatly attached to an aluminum plate. This plate has a 10″ circle etched on it to mark where the electron beam will strike and expose the samples. The aluminum plate is attached to the system's water-cooled backplate, and a thermocouple is connected to the backplate to monitor the temperature. A Faraday cup is also placed on the backplate to monitor electron dosage rate. The water-cooling system keeps the samples from overheating during irradiation. The maximum temperature that the samples experienced was 100° F (38° C), and generally, the tem-
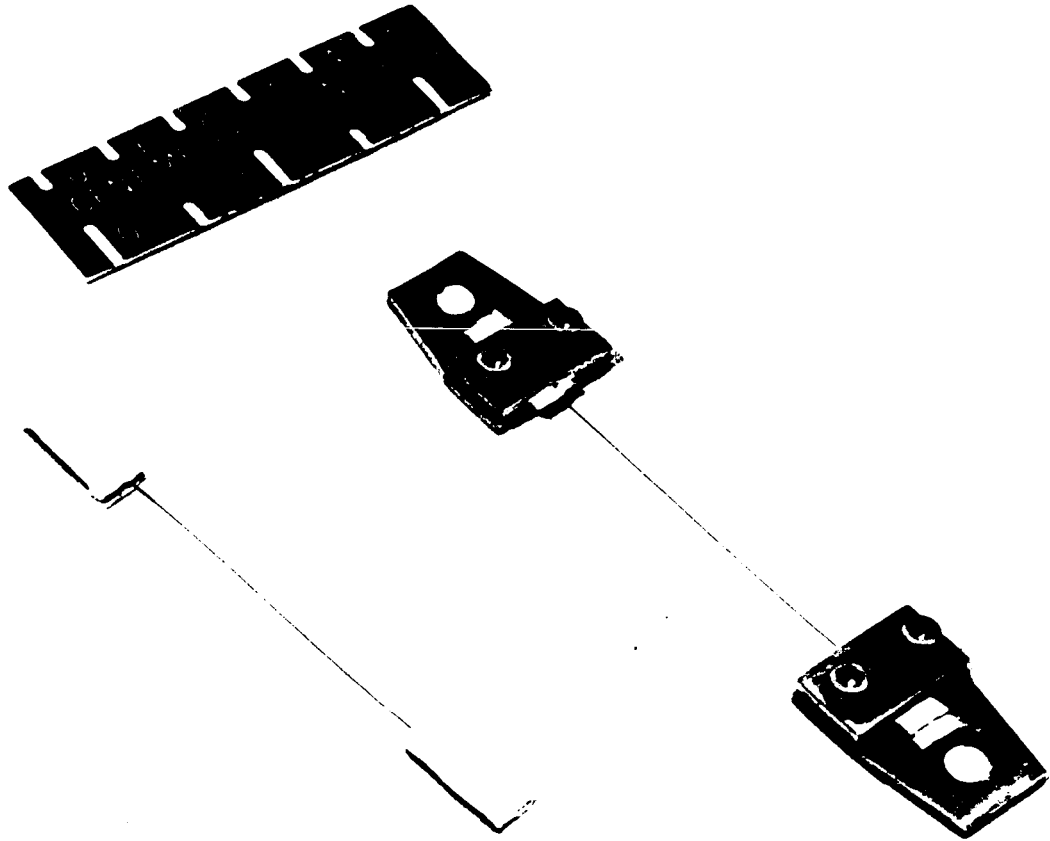
Figure 7.   Tabbed Fibers and Test Grips

perature was around 95° F. There was no temperature difference between the back and front surfaces of the specimen during irradiation.

2.2.2 Mechanical Testing

Tension tests at LaRC were conducted on an Instron machine equipped with an environmental chamber. The mechanical grips in which the coupons were mounted fit entirely within this chamber. Both room temperature (75° F/24° C) and elevated temperature (250° F/121° C) tests were conducted. Heat was generated from resistance elements and circulated by an internal fan. The temperature was monitored by means of a thermocouple attached to the specimen and other thermocouples placed about the chamber. The load cell was located outside the chamber and isolated from temperature variations. Load was introduced at a constant crosshead speed of 0.02"/minute (0.5 mm/min.) and measured by a resistance load cell. The specimen gripping fixture was attached to the load cell by means of a universal joint located at the top of the load train. Stress data, along with strain data, were collected and recorded by a computerized data acquisition system.

Tension testing at Virginia Tech was performed on a United Testing Systems (UTS) screw-driven, displacement controlled testing machine. An oven, which enclosed the rotating test grips, was mounted on the machine for elevated temperature tests, and heat was generated by resistance elements and circulated by an internal fan. The grips used were designed to reduce shear coupling effects and eliminate alignment problems [5]. Temperature was monitored, as above, by thermocouples. As was the set-up at LaRC, the resistance load cell was located outside the test chamber and data were sampled and recorded by a computerized data acquisition system.

An Instron test machine with a maximum resistance load cell of 10 lbs. (4.5 kg.) was used to test single graphite fibers at LaRC. The constant displacement rate tests were all run at room temperature. Load and strain were determined during each test as a function of time. The load-time graph

was determined from the load cell and the displacement from a linear vertical displacement transducer (LVDT).

2.3 Test Methods

2.3.1 Coupon Tension Tests

Two types of tension tests were performed. One was a monotonic test, where the coupon was loaded continuously until failure and properties found as noted previously. The other was a cyclic test where the coupon was loaded beyond the linear region, then unloaded until there was zero load present, and finally reloaded until failure. Specimens tested during early portions of this study were cycled as many as three times at various stresses. All loading and unloading was performed at a constant crosshead speed. The test matrix for all monotonically and cyclically loaded specimen is shown in Table 2. No cyclic tests for $[0]_4$ coupons were run as the effects of radiation on the fiber-dominated properties were small and the material unloaded elastically. From the cyclic tests of the $[10]_4$, $[45]_4$ and $[90]_4$ coupons, the non-linear response, permanent strain and energy dissipation of the material can be characterized. A cyclic test schematic is presented in Fig. 8. The shaded area is equivalent to the amount of energy dissipated into heat per cycle [6]. The strain present at zero stress after unloading is the permanent set or permanent strain. Energy dissipation may be due to factors such as fiber breakage, fiber/matrix interface debonding, matrix crazing, matrix plasticity or void and crack formation. Degradation of the material will be defined as a breakdown in the material chemistry, due to the space environmental parameters and observed as lowered strength and stiffness. Occurrences of proportional limits lower than that of the room temperature tested baseline material are also considered to be matrix degradation.
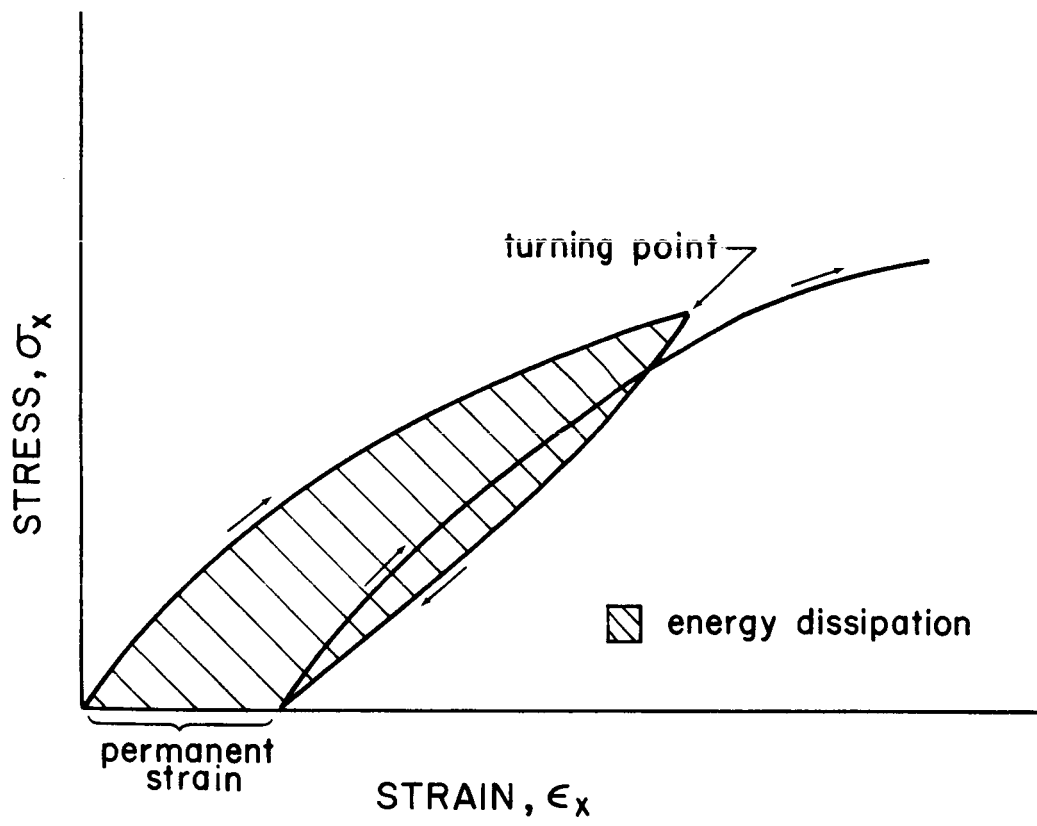
Figure 8. Cyclic Tension Test Schematic

2.3.2 Single Fiber Tests

Tension tests of graphite fibers were conducted at a crosshead speed of 0.05″/minutes (1.3mm/min.). Strain and load were measured as a function of time. From these data, the ultimate strength and elastic modulus were determined. Data for baseline and irradiated samples were then compared to examine the effects of radiation on graphite fibers.

2.3.3 DMA and TMA

Dynamic-Mechanical Analysis (DMA) was used to obtain the damping characteristics and the dynamic modulus of elasticity as a function of temperature. A detailed explanation of the DMA and TMA techniques used are given by Milkovich et al. [2] and Sykes et al. [3]. Data were recorded from -184° F (-120° C) up through the glass transition temperature (T_g) at a rate of 9° F/min (5° C/min). The $[90]_4$ samples were used for the DMA tests so that the data would primarily reflect matrix properties. From these tests, the T_g of the baseline and irradiated materials, both modified and standard, were determined. This technique is very useful for comparing the temperature dependent characteristics of various resin matrix composites.

Thermomechanical Analysis (TMA) gives information concerning phase transitions, softening points, modulus changes and creep properties of a material. This is also a useful method for determining changes in temperature dependent properties. The test is performed by placing a hemispherical tipped Quartz probe on a sample of material and loading to a given weight. The penetration of the probe is measured and recorded with respect to the temperature.

2.3.4 Post Failure Analysis

Additional information concerning the failure mechanisms of the coupons were obtained using scanning electron microscope (SEM) and X-ray techniques. SEM micrographs of the $[45]_4$ coupon fracture surfaces (both baseline and irradiated materials from room temperature and elevated temperature tests) were examined to study the differences in the failure modes. The fracture surfaces were coated with gold-palladium prior to SEM inspection to reduce charging effects. X-ray photographs were taken of the failed $[45]_4$ irradiated and non-irradiated coupons. These specimens were first dyed with a zinc oxide solution and then X-rayed to determine if any microcracking had occurred.

3.0 Results and Discussion

The results of the tests performed for this study will be presented in four parts:

- The effects of electron irradiation and temperature on in-plane mechanical properties of the modified graphite-epoxy composite system as determined from monotonic tension tests (Section 3.1).

- The effects of irradiation and temperature on the energy dissipation of the composite material as determined from cyclic tests (Section 3.2).

- The effects of irradiation and temperature on the epoxy matrix (Section 3.3).

- The effects of irradiation and temperature on the graphite fiber as determined from the single fiber tension tests (Section 3.4).

A discussion of possible chemical structure changes in the material which would account for the above results is presented in section 3.5.

Comparisons of the modified material behavior to that of the standard T300/934 graphite-epoxy composite material will be discussed in section 3.6.

3.1 Monotonic Tests

The specimens used for both monotonic and cyclic tests were cut from eight unidirectional, 4-ply panels. The ultrasonically C-scanned panels were found to be without voids or cracks. Each panel was found to be non-uniform in thickness, varying as much as 0.004" (0.102 mm), with the nominal thickness for each panel being between 0.020" (0.508 mm) and 0.023"(0.584 mm). Specimens of each orientation were cut from the same panel, except in the case of the [45]$_4$ specimens. The [45]$_4$ coupons were first cut from panel A. As fewer [45]$_4$ coupons can be obtained from a panel than any other orientation, it was necessary to cut a second group from panel B. The first group was tested at LaRC and the second at Virginia Tech. Therefore these results are presented separately when possible.

Failed coupon specimens for each orientation of the modified T300/934 graphite-epoxy composite system are pictured in Fig. 9. Typical axial stress-strain results of the modified material monotonic tension tests are presented in Figs. 10, 12, 14 and 16. Transverse strain versus axial strain results for [0]$_4$ laminates are presented in Fig. 11. The off-axis [10]$_4$ and [45]$_4$ test results are presented in Figs. 13 and 15 in terms of shear stress versus shear strain. In each figure, both baseline room temperature tested and elevated temperature tested results are presented, along with irradiated room temperature tested and elevated temperature tested results. Average experimental values for mechanical properties are quoted in the text and presented in Table 3. Additional test data is presented Appendix B.

[0]$_4$ laminates

Initial [0]$_4$ tests were conducted with fiberglass tabs bonded to the specimens with a standard room temperature curing epoxy adhesive. During tension testing at high loads or high temperatures this adhesive tended to disintegrate causing the the tabs to slip from the specimens. Various epoxies and coupon gripping methods were then tried in order to resolve the problem. Applying the tabs
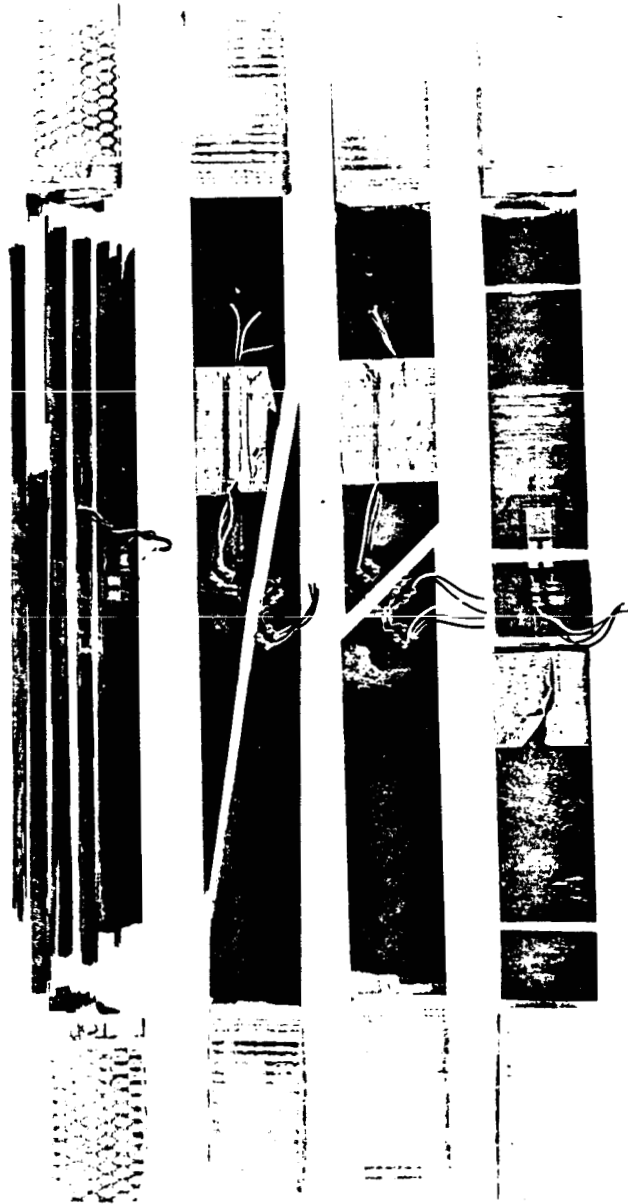
Figure 9. Failed Tension Test Coupons

Results and Discussion

24

Table 3. Experimental In-Plane Mechanical Properties of Modified T300/934 Graphite-Epoxy

Orientation/Property		Room-BSL	Room-IRR	Elev-BSL	Elev-IRR
$[0]_4$	E_1 (msi)	21.0	20.6	22.2	23.6
	v_{12}	0.345	0.312	0.355	0.371
	X_T (ksi)	211.	235.	---	206.
	$\varepsilon_{1_{ult}}$ (%)	0.973	1.09	---	0.885
$[10]_4$	E_x (msi)	12.3	12.5	11.3	9.97
	G_{12}^* (msi)	0.803	0.793	0.668	0.517
	G_{12}^+ (msi)	0.831	0.908	0.701	0.527
	S (ksi)	10.1	10.1	7.11	4.32
	$\varepsilon_{x_{ult}}$ (%)	0.584	0.812	0.624	0.567
$[45]_4$	E_x (msi)	1.87	2.06	1.63	1.31
	G_{12} (msi)	0.683	0.752	0.569	0.422
	$\varepsilon_{x_{ult}}$ (%)	1.10	1.18	1.27	0.725
$[90]_4$	E_2 (msi)	1.23	1.51	1.18	0.880
	Y_T (ksi)	8.08	6.84	6.86	4.67
	$\varepsilon_{2_{ult}}$ (%)	0.680	0.442	0.614	0.654

Room--Room Temperature Tested   *--Experimental (apparent) values
Elev--Elevated Temperature Tested   + --Pindera and Herakovich apparent value predictions
BSL--Baseline Material
IRR--Irradiated Material

with a 350° F (177° C) curing adhesive was the best solution. This method required the coupon ends to be heated to 450° F (232° C) for four minutes. Although this caused some blistering near the tab area of the irradiated specimens, it did not appear to adversely affect the tests. This method of tab adhesion was not the final solution to the problem as some tab slippage still occurred. For this reason, the strength data for the modified material system is incomplete.

Typical stress-strain results for the $[0]_4$ coupons are shown in Fig. 10. The data show that the axial stress-strain behavior is fairly linear, but does exhibit the stiffening behavior typical of $[0]_4$ graphite-epoxy. The average elastic moduli for the baseline and irradiated room temperature tested materials are nearly equal (21.0 msi and 20.6 msi, respectively). The elevated temperature tested materials have higher elastic moduli, an average of 5.6% for the baseline material and 11.5% for the irradiated material as compared to the room temperature tested baseline material (Table 3). The higher initial moduli for the elevated temperature tested materials is believed to be primarily due to reduced residual stresses in the matrix, as graphite fibers are unaffected by temperatures in the testing range [7]. Further degradation of the matrix due to irradiation allows a greater reduction of residual stresses and therefore increased composite stiffness. The radiation-induced material changes that cause these phenomena are discussed in section 3.5.

As noted before, many of the $[0]_4$ specimens did not fail. Therefore, the strength for all cases is not thoroughly tested. Specimens that did reach failure loads without tab slippage are noted in Appendix B. These tests indicate that the strength, X_T, of the failed specimens is an average of 213 ksi (1470 MPa), but ranges as high as 235 ksi (1620 MPa).

From the $[0]_4$ tests, Poisson's ratio, v_{12}, was determined. Typical results of the negative transverse strain, ε_2, to the axial strain, ε_1, are presented in Fig. 11. These results show no significant change in Poisson's ratio between room and elevated temperature tested or baseline and irradiated materials (Appendix B). Poisson's ratio is often assumed as a constant for unidirectional composites, because it is not a sensitive micromechanical variable [8]. The average v_{12} value of all fifteen tests is 0.358 with the average for each case being within 3.6% of that value.

Figure 10. Modified [0]₄ Monotonic Tension Stress-Strain Results
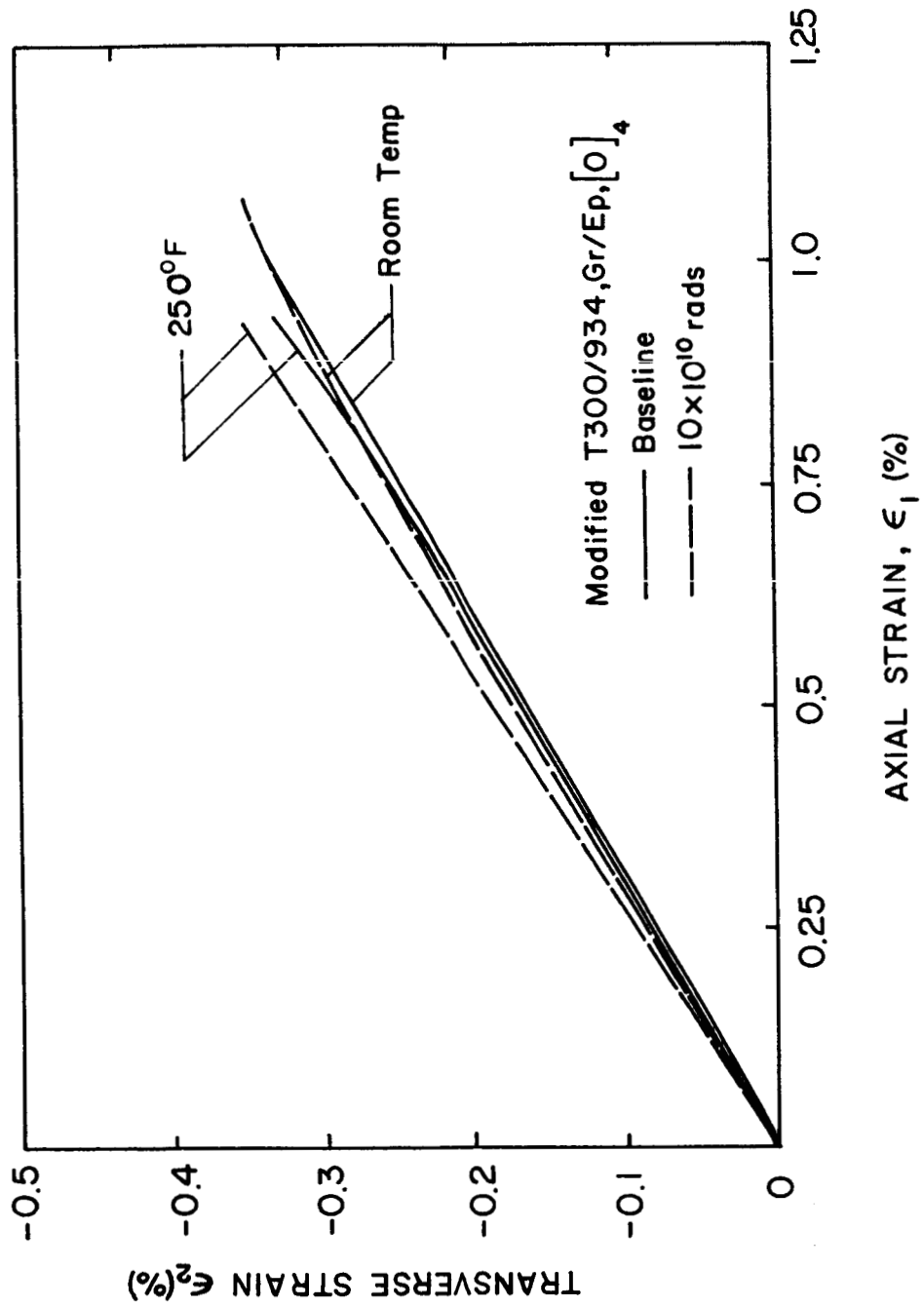
Figure 11. Modified [0]₄ Monotonic Tension Transverse Strain-Axial Strain Results

[10]₄ laminates

Axial Response

Figure 12 shows typical axial stress-strain curves for the [10]₄ coupons. The room temperature baseline and irradiated materials show nearly equal elastic moduli (averages of 12.3 and 12.5 msi, respectively) and ultimate stresses (averages of 59.2 and 60.0 ksi, respectively). The irradiated material, though, exhibits increased non-linearity and a 39% greater ultimate strain when compared to the baseline material at room temperature. Elevated temperature tests show lower moduli, 33% for the baseline material and 50% for the irradiated material, as compared to the room temperature tested baseline material. The tests at the elevated temperature also exhibit increased non-linearity and significantly lowered ultimate stresses. The results in Fig. 12 show that at both test temperatures, irradiation causes significantly lower proportional limits and increased non-linearity, apparently due to degradation of the material.

Shear Response

Typical apparent shear stress-shear strain results from the [10]₄ laminate tests are presented in Fig. 13, and the average experimental shear modulus values, G_{12}^*, are presented in Table 3. Also shown in Table 3 are values of G_{12}^+, where G_{12}^+ is the prediction for G_{12}^* based upon the analysis of Pindera and Herakovich [9]. It is apparent from Table 3 that the experimental G_{12}^* and predicted G_{12}^+ are well within the range of acceptable correction considering the idealizations inherent within the analysis and experimental error. The room temperature tested materials exhibit nearly equal initial shear moduli (averages of 0.803 msi for the baseline material and 0.7931 msi for the irradiated material, Table 3). The baseline and irradiated elevated temperature tests show 17% and 36% lower shear moduli, respectively. The baseline and irradiated room temperature tests have identical shear strengths, S, (averages of 10.1 ksi), but the irradiated material exhibits a 71% higher shear strain at failure when compared to the baseline material. The ultimate shear stress of the elevated temperature tested baseline material is 30% less than the room temperature baseline material, but exhibits
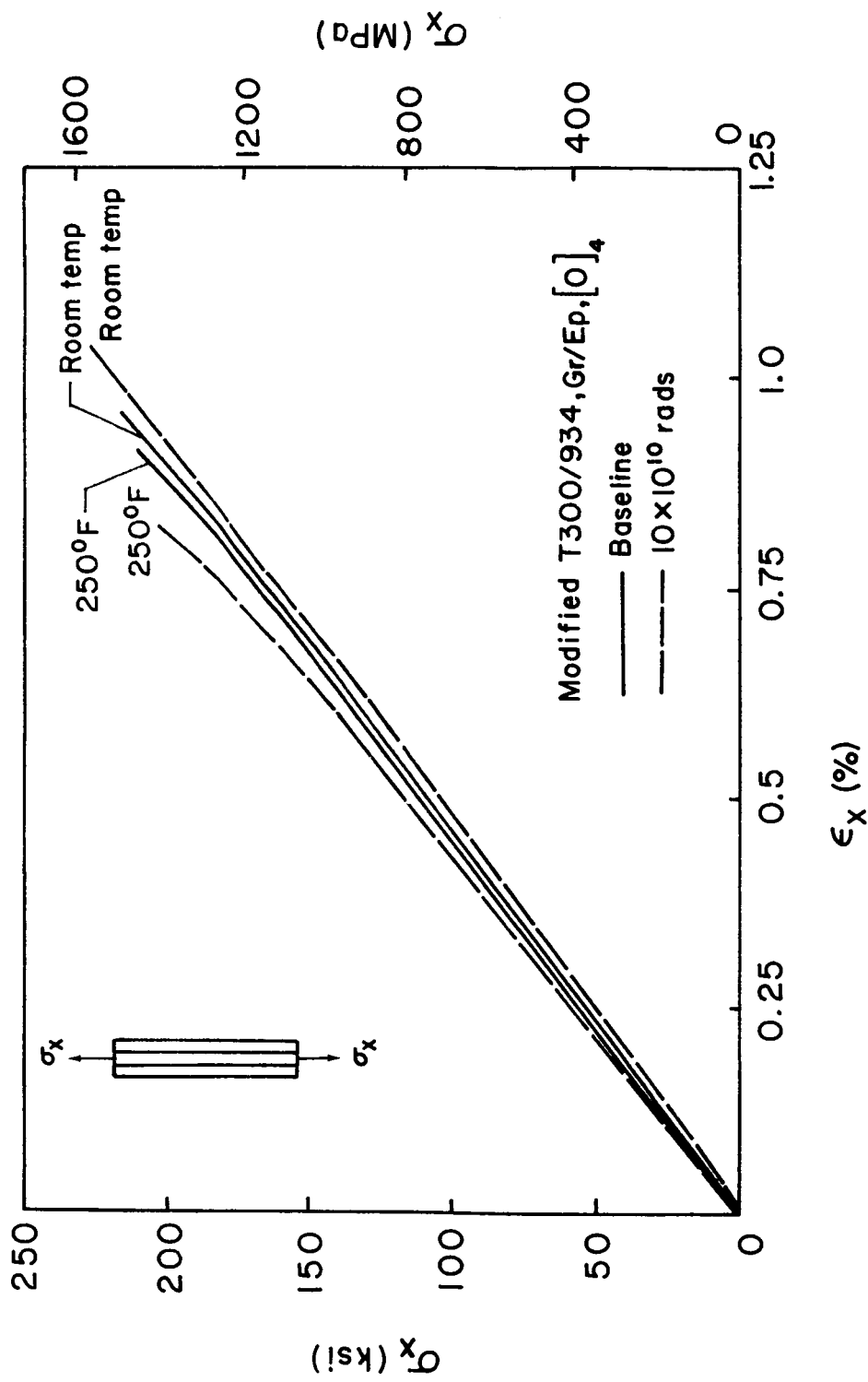
Figure 12. Modified [10]₄ Monotonic Tension Stress-Strain Results
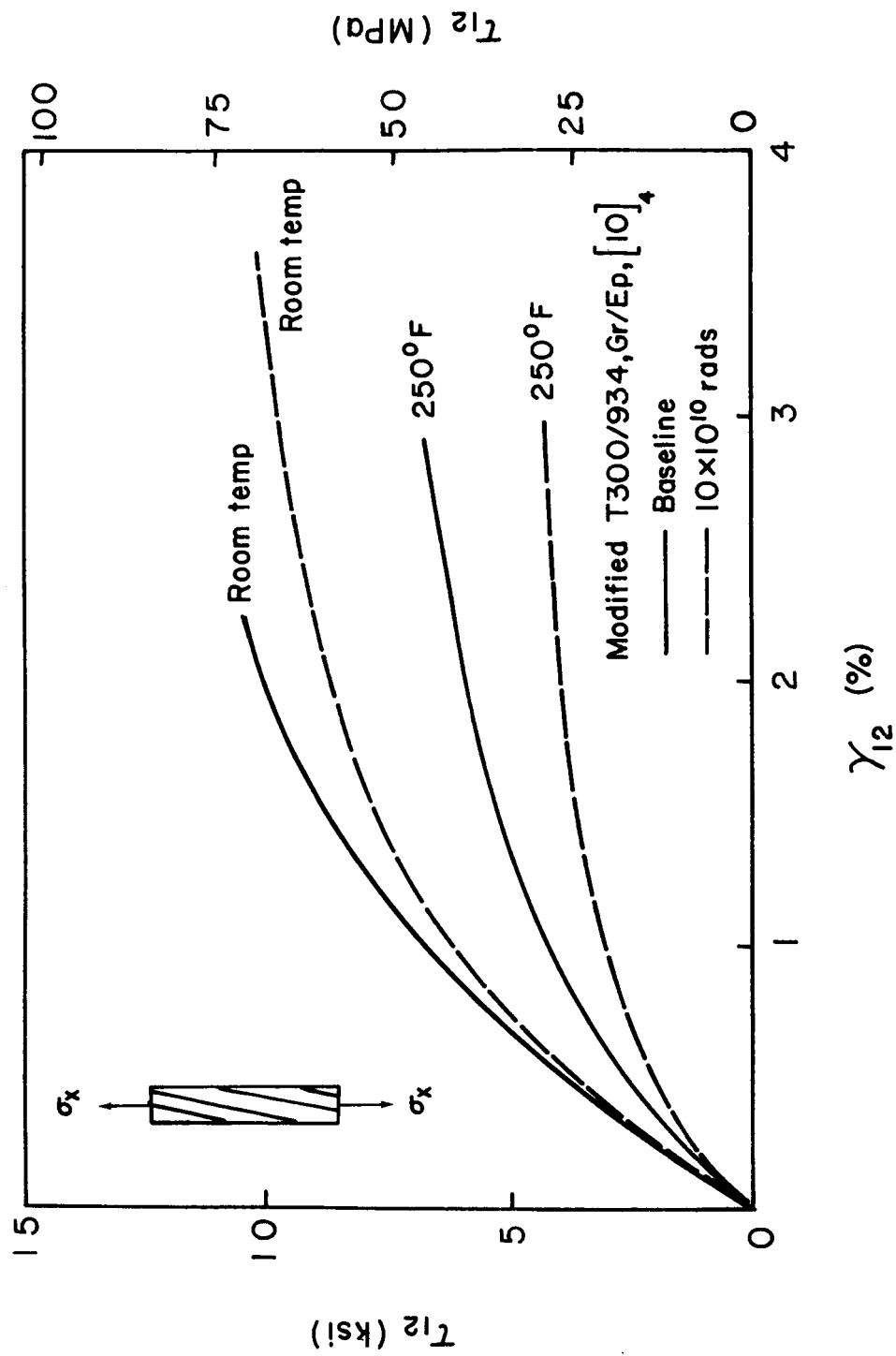
Figure 13. Modified [10]$_4$ Monotonic Shear Stress-Shear Strain Results

a 47% increase in shear strain at failure. The elevated temperature tested irradiated material shows a 57% decrease in ultimate shear stress from the room temperature tested baseline material, but a 33% higher ultimate shear strain. The ultimate shear strain values presented for the elevated temperature tested materials are the minimum values as strain gage failure occasionally occurred just prior to material failure. An explanation of the possible matrix changes which cause the above results can be found in section 3.5.

[45]₄ laminates

Axial Response

Typical axial stress-strain curves for the [45]₄ laminates tested at LaRC, presented in Fig. 14, show the increased matrix domination in the behavior of these specimens (average property values of these tests are presented in Table 3). The irradiated material at room temperature, exhibits a 10% higher initial axial modulus than the baseline material average of 1.87 msi, and a slight increase of non-linearity at the higher stresses. Elevated temperature tests show a 26% decrease in the initial modulus for the baseline material and a 57% decrease for the irradiated material as compared to the room temperature baseline material results. The elevated temperature tested baseline material also exhibits a 30% higher ultimate strain than the room temperature baseline material. The effects of degradation in this elevated temperature tested irradiated material are seen in the 57% lowered failure strength.

Shear Response

Typical curves for the [45]₄ shear stress-shear strain tests conducted at LaRC are presented in Fig. 15. The initial shear modulus, G_{12}, of the room temperature tested irradiated material is an average of 10% higher than that of the room temperature tested baseline material (0.683 msi). The moduli of the elevated temperature tests, baseline and irradiated materials, show 17% and 38% decreases, respectively. For every [45]₄ room temperature test, note that though the irradiated material has a
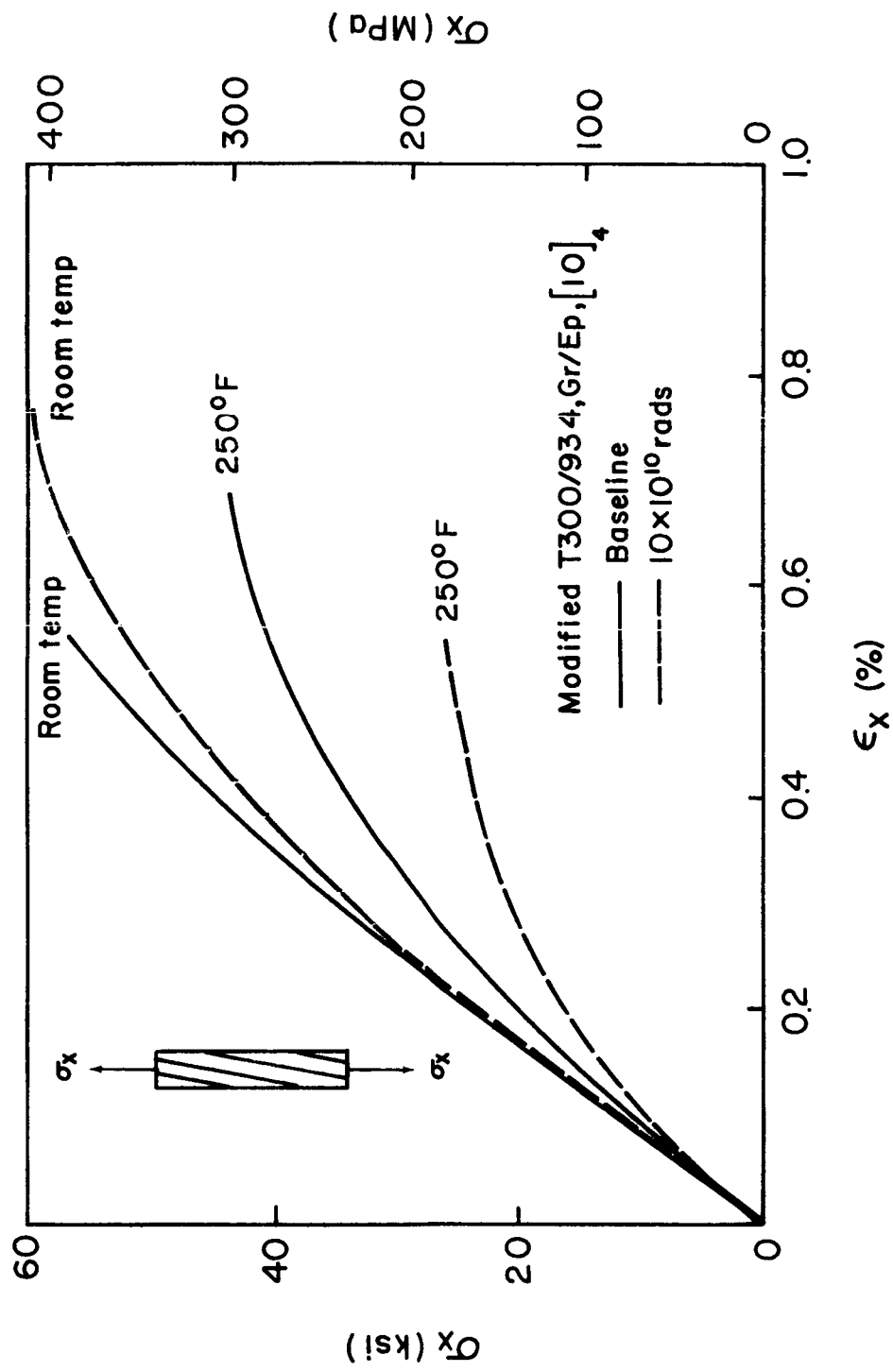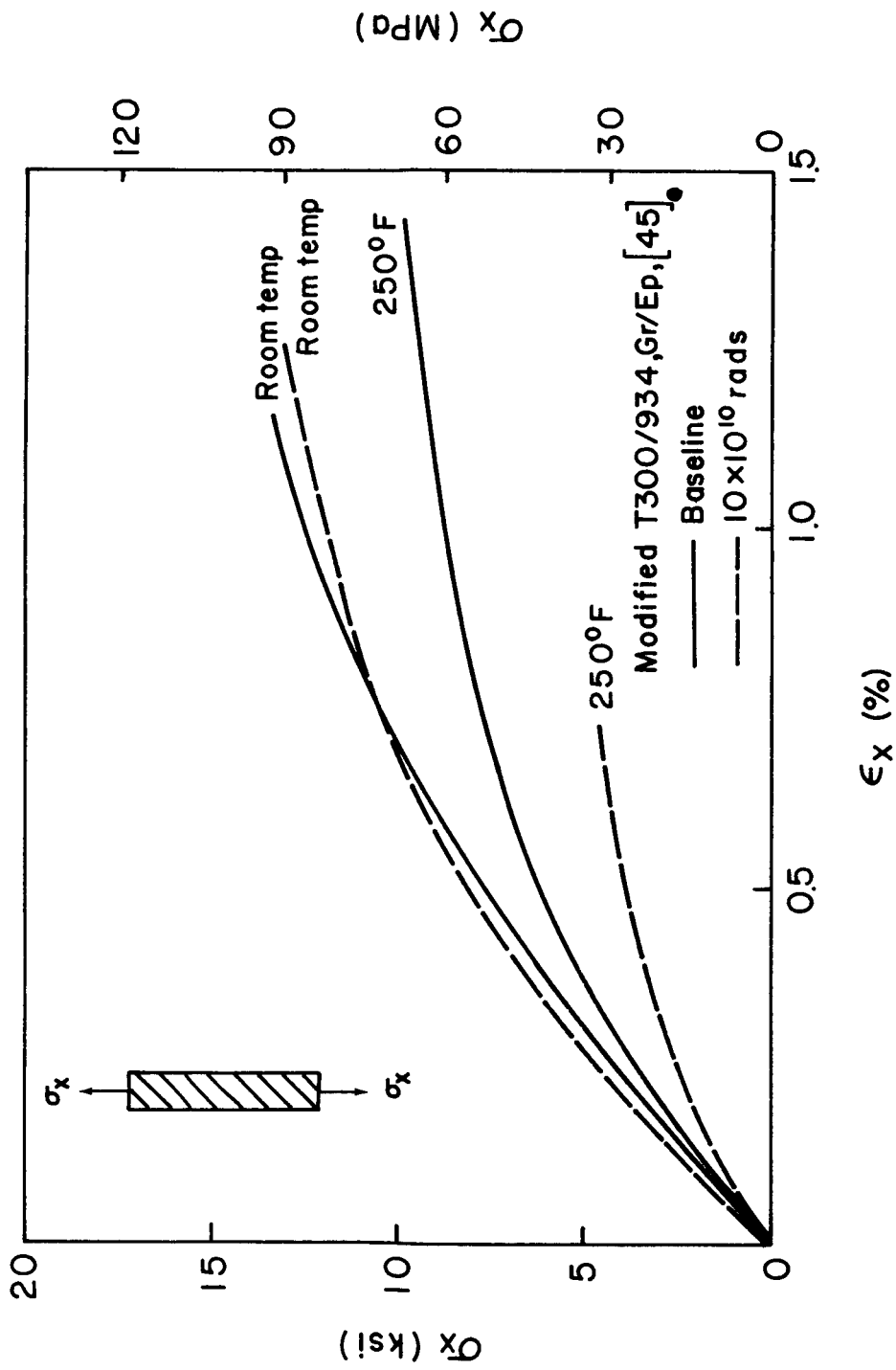
Figure 14. Modified [45]₄ Monotonic Tension Stress-Strain Results
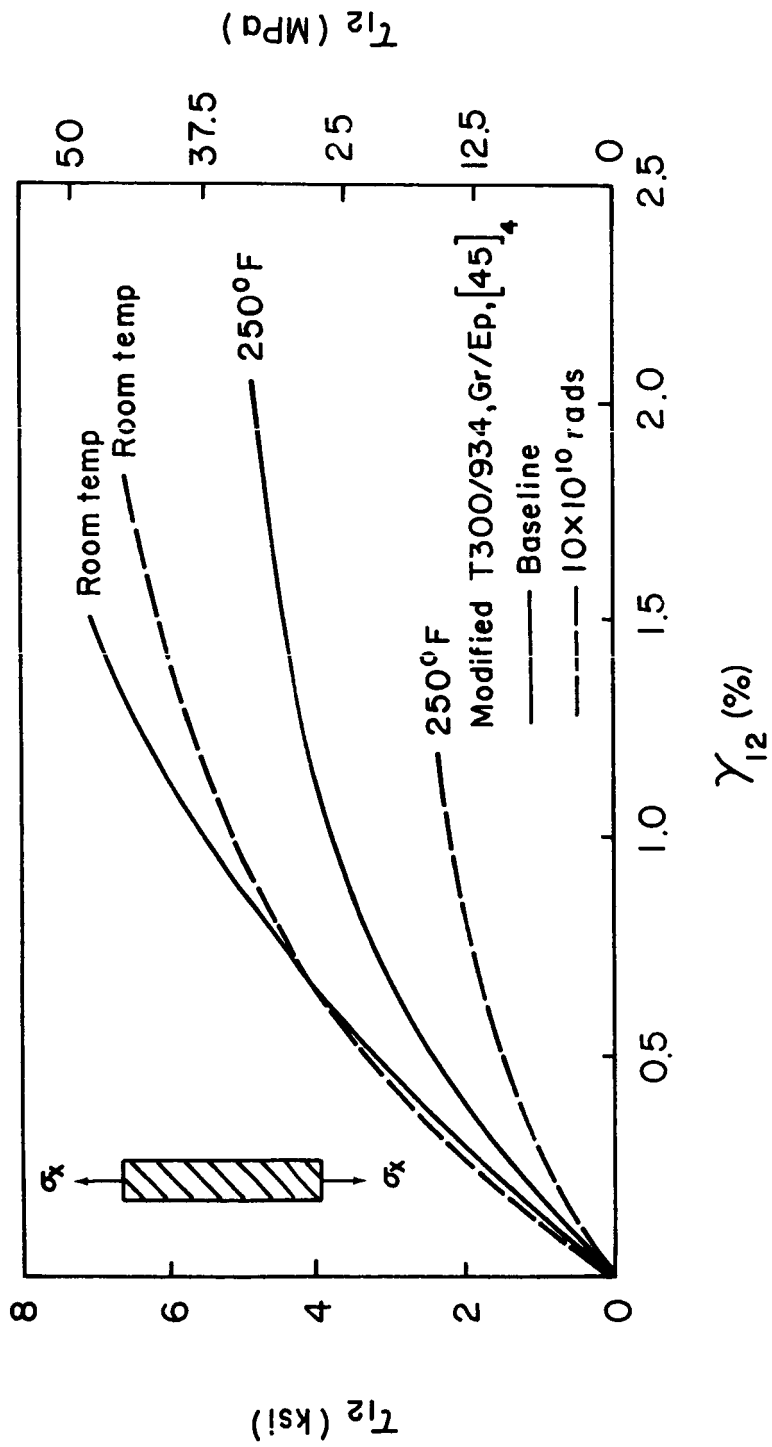
Figure 15. Modified |45]₄ Monotonic Shear Stress-Shear Strain Results

higher initial shear modulus, the material exhibits increased ductility. The proportional limit is lower, but the strain to failure is higher. The room temperature irradiated material also exhibits a 10% lower shear stress at failure than the baseline material. The elevated temperature tested baseline material fails at a 30% lower shear stress than the room temperature baseline material, but at a 28% greater shear strain. The elevated temperature tested irradiated material exhibits both a 66% lower shear stress and a 27% lower shear strain when compared to the room temperature baseline results. These $[45]_4$ laminates fail due to the transverse stress, σ_2 , and the shear stress, τ_{12}. Therefore the failures exhibited for the $[45]_4$ specimens at a given shear stress are not pure shear failures.

Shear Response Comparison of $[10]_4$ *and* $[45]_4$ *Laminates*

Comparing the shear stress-shear strain results of the $[10]_4$ and $[45]_4$ tests (Figs. 13 and 15), notice that the shear moduli of the $[10]_4$ laminates is higher than that of the $[45]_4$ laminates. Shear stresses and shear strains at failure are also higher for the $[10]_4$ specimens. The $[10]_4$ laminates primarily fail due to the shear stress, τ_{12}, where the failure of the $[45]_4$ laminates is due to a combination of the shear stress and the transverse stress component, σ_2. The shear results presented are from the apparent shear stresses, as the assumption that $\sigma_y = \tau_{xy} = 0$ (Appendix A.1) was used.

$[90]_4$ **laminates**

Typical curves for the $[90]_4$ specimen are presented in Fig. 16. All responses are initially linear but exhibit non-linearity with increased stress. The behavior of the baseline material is typical of this type of epoxy [10]. The room temperature tested irradiated material exhibits the highest initial transverse elastic modulus, E_2 (an average of 23% greater than the room temperature baseline material's average of 1.23 msi). The elevated temperature tests exhibit a lower elastic moduli than the room temperature baseline tests (4.5% for the baseline material and 29% for the irradiated material).
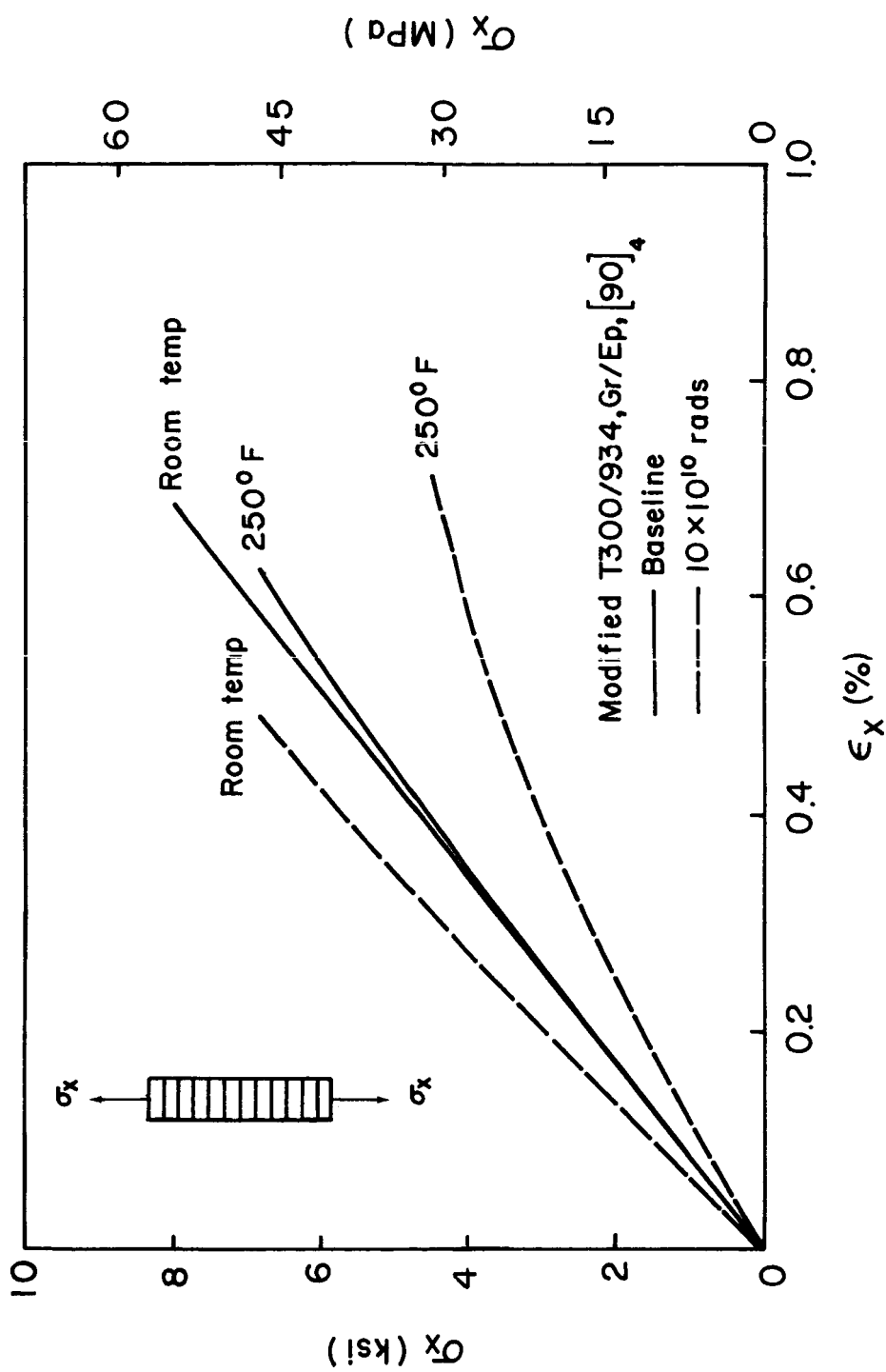
Figure 16. Modified |90|₄ Monotonic Tension Stress-Strain Results

The highest strength, Y_T, is exhibited by the room temperature baseline material. Failure occurred at an average stress of 8.08 ksi. The room temperature irradiated material and the elevated temperature baseline material fail at 85% of the room temperature baseline strength value. The irradiated elevated temperature tested material fails at 58% of the room temperature baseline value. The average failure strain of the elevated temperature irradiated material, though, is only 4% less than that of the room temperature baseline material, whereas the elevated temperature tested baseline material failure strain is 10% lower, and that of the room temperature irradiated material is 35% lower.

3.2 Cyclic Tests

3.2.1 Single Cycle Tests

Cyclic tests were conducted for the $[10]_4$ and $[45]_4$ modified material laminates at room and elevated temperatures, and for the $[90]_4$ coupons at the elevated temperature. Typical axial stress-strain curves are shown in Figs. 17, 19 and 21, and typical shear stress-shear strain curves are presented in Figs. 18 and 20.

$[10]_4$ **laminates**

Axial Response

The irradiated material, at both room temperature and elevated temperature (Figs. 17c and 17d), exhibits a greater amount of energy dissipation and permanent strain than their baseline equivalents (Figs. 17a and 17b). Also, the irradiated material does not reload through the turning point of the

a) Room Temperature Tested - Baseline Material

b) Elevated Temperature Tested - Baseline Material

c) Room Temperature Tested - Irradiated Material

d) Elevated Temperature Tested - Irradiated Material
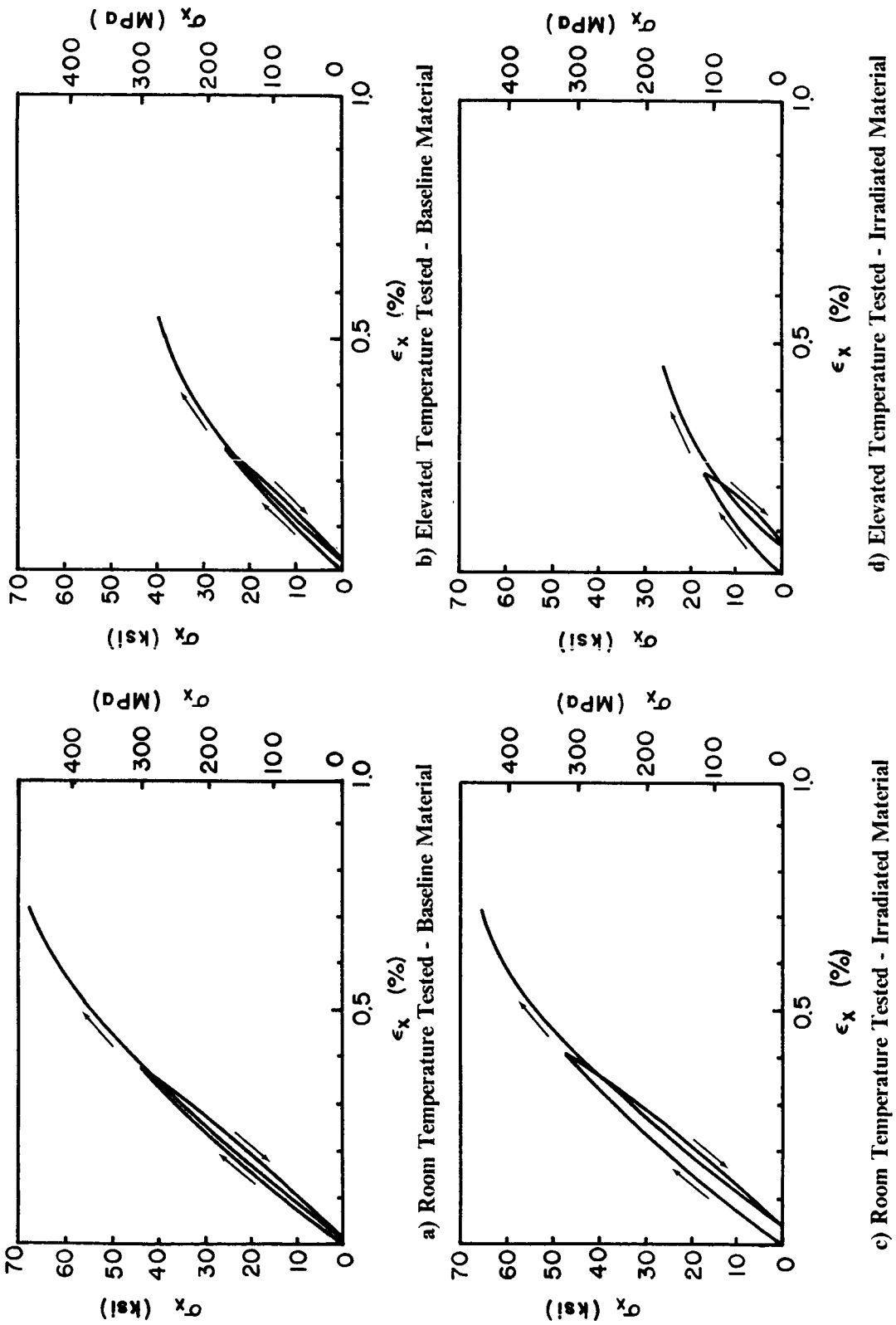
Figure 17. Modified |10|₄ Cyclic Tension Stress-Strain Results

previous cycle. These effects are more pronounced for the elevated temperature irradiated material than the room temperature irradiated material.

The energy dissipation is a combination of time dependent and time independent deformation. It is uncertain whether the irradiated material exhibits an increased amount of plastic, viscoelastic or both types of deformation when compared to the baseline material. In general, polymer matrix composite materials are viscoelastic, and it is believed that the irradiation produced low molecular weight products plasticize the material in a time dependent manner. The curves also show many of the trends noted for the monotonic tests.

Shear Response

The cyclic shear stress-shear strain curves are presented in Fig. 18. These curves exhibit the same behavior as the axial stress-strain curves. However, from the shear tests, it is easier to see that irradiation causes more energy dissipation in the material than elevated temperature. Possible changes in the material which result in the above behavior are discussed in section 3.5.

$[45]_4$ laminates

Axial Response

A significant increase of energy dissipation and permanent strain is exhibited by the irradiated materials (Figs. 19c and 19d) when compared to their baseline equivalents (Figs. 19a and 19b). Also upon cycling, the irradiated materials do not reload through the previous unloading point of the curve. These results, which are more matrix dominated than those of the $[10]_4$, show the increased effect of epoxy degradation due to irradiation. When comparing other parameters between the $[45]_4$ materials, it should be noted that the room temperature tests were performed at LaRC and the elevated temperature tests were performed at Virginia Tech.

Shear Response

b) Elevated Temperature Tested - Baseline Material

d) Elevated Temperature Tested - Irradiated Material

a) Room Temperature Tested - Baseline Material

c) Room Temperature Tested - Irradiated Material
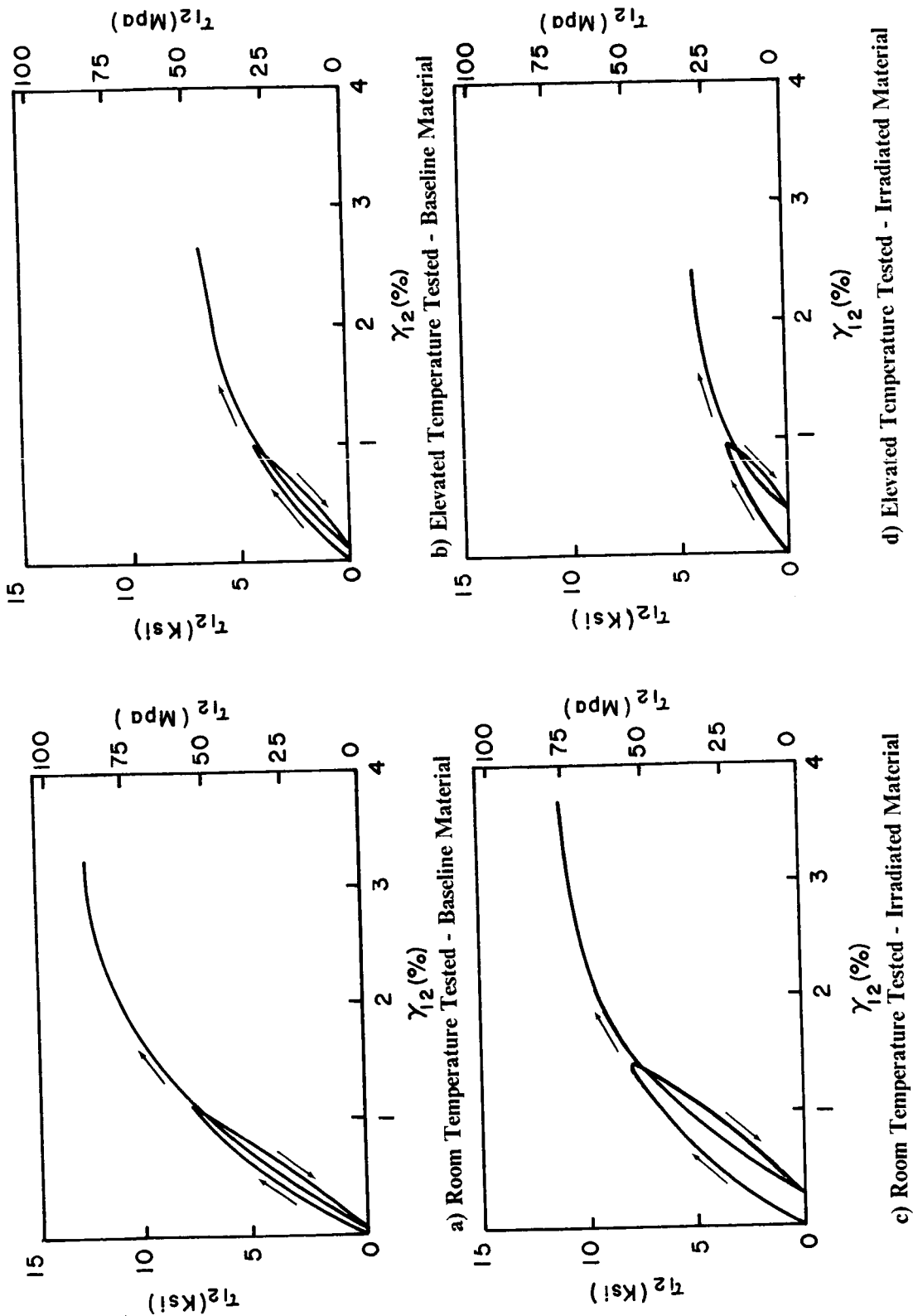
Figure 18. Modified [10]₄ Cyclic Shear Stress-Shear Strain Results
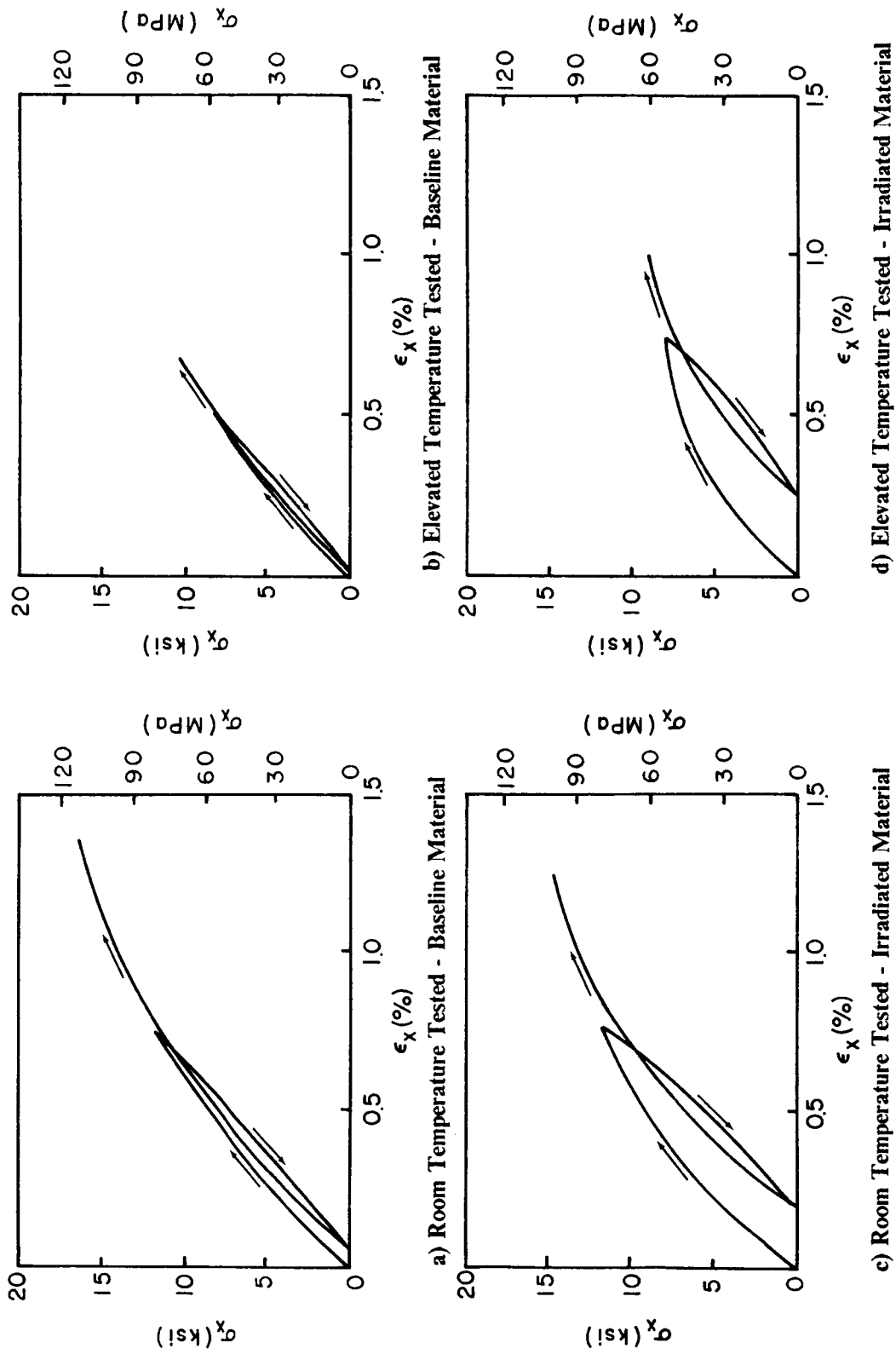
Figure 19. Modified |45|₄ Cyclic Tension Stress-Strain Results

The results in terms of shear stress versus shear strain (Fig. 20) show very similar trends to the axial stress-strain results. Much of the permanent strain and the fact that the irradiated materials do not reload through the previous point of unloading, are believed to be time dependent phenomena.

[90]₄ laminates

The [90]$_4$ elevated temperature tested baseline material (Fig. 21a) shows no energy dissipation for the level of loading considered. The material unloads and reloads along the original loading curve. The irradiated material exhibits energy dissipation and permanent strain (Fig. 21b), and does not reload through the turning point. These matrix dominated tests clearly show the increased energy dissipation due to irradiation coupled with elevated temperatures. Additional tests are required to determine the plastic or viscoelastic nature of these effects.

3.2.2 Multiple Cycle Tests

Multiple cycle tension tests were conducted on [45]$_4$ laminates. These materials were cycled first at 0.2% axial strain, then successively at 0.3%, 0.4%, 0.5%, and 0.6% strain, and finally loaded to failure.

The successive loadings of each multiple cycle test showed no significant change in the initial shear nor axial modulus. Typical tests in terms of shear stress versus shear strain are presented in Figs. 22 and 23. Loadings only are presented for each case in Fig. 24, where each successive loading is offset by 0.1% shear strain. Unloadings only are also presented in this manner in Fig. 25. Unloadings in all of the [45]$_4$ cases show a decrease in initial unloading elastic and shear moduli for each successive cycle. The room temperature tested irradiated material (Fig. 25c) exhibits a 9% decrease of initial shear modulus from the first to the last unloading. The moduli of all of the other materials decreased approximately twice as much (18% for the room temperature baseline material

b) Elevated Temperature Tested - Baseline Material

d) Elevated Temperature Tested - Irradiated Material

a) Room Temperature Tested - Baseline Material

c) Room Temperature Tested - Irradiated Material
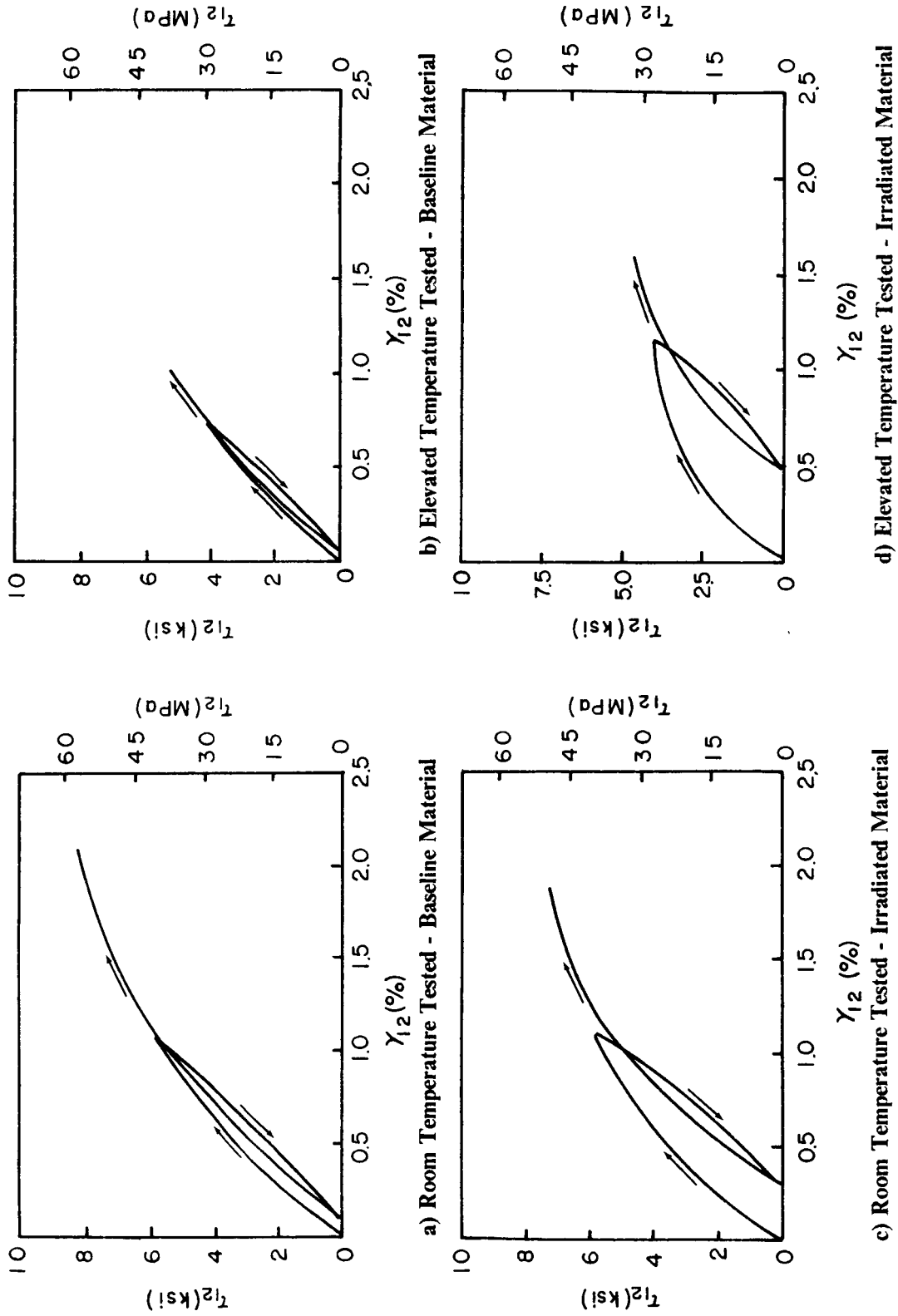
Figure 20.   Modified |45|₄ Cyclic Shear Stress-Shear Strain Results
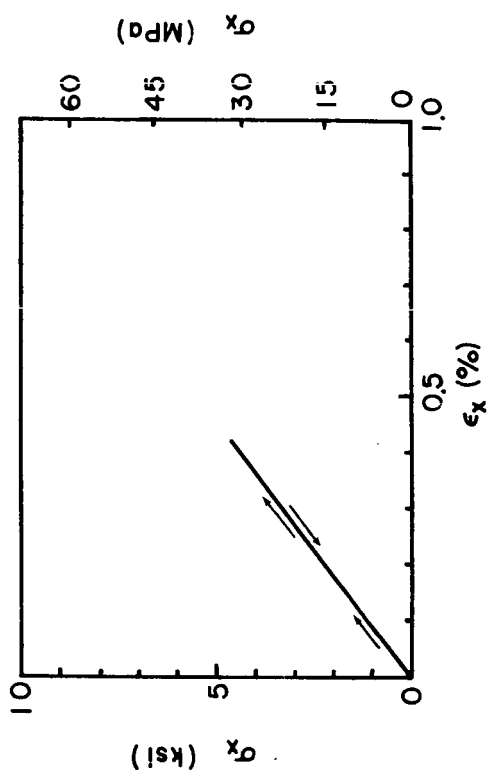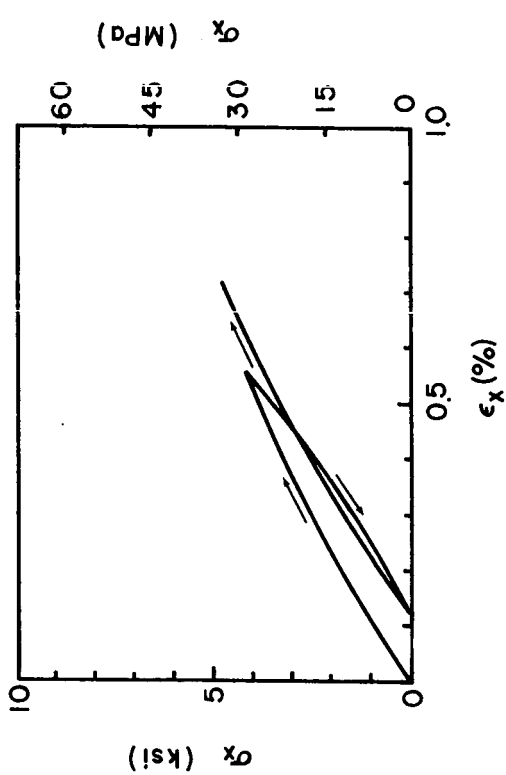
Figure 21.   Modified [90]₄ Cyclic Tension Stress-Strain Results

a) Elevated Temperature Tested - Baseline Material

b) Elevated Temperature Tested - Irradiated Material
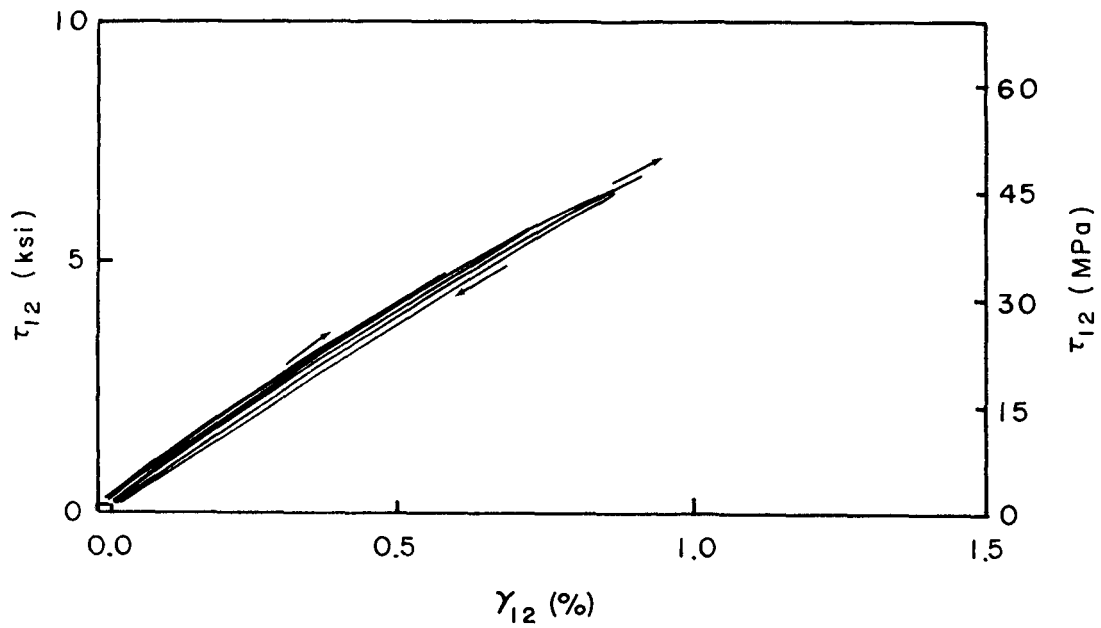
a) Room Temperature Tested - Baseline Material
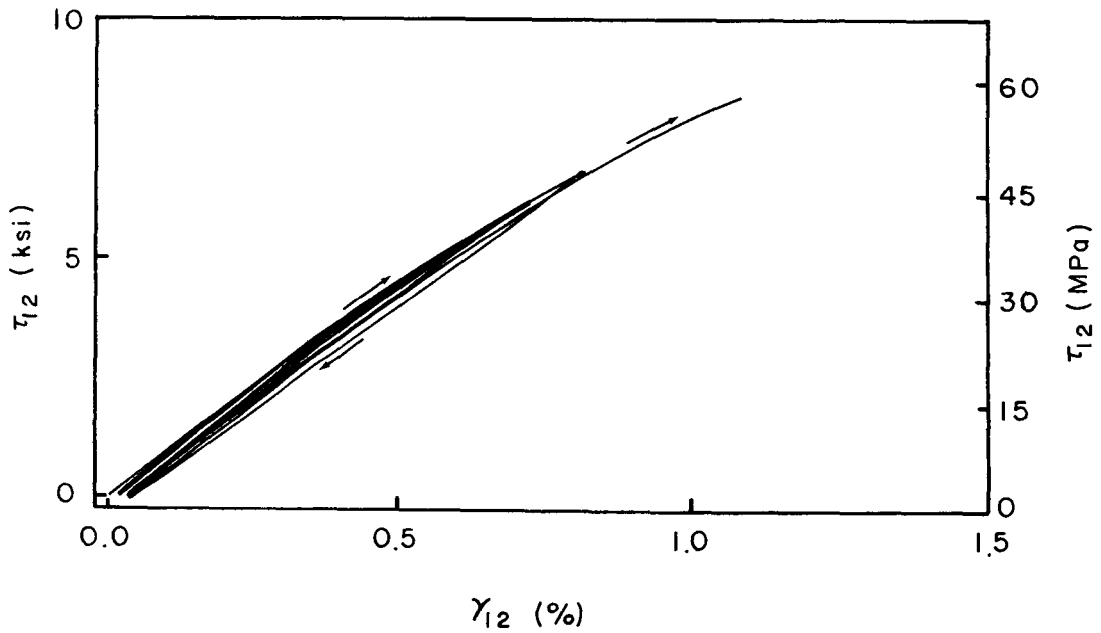
b) Room Temperature Tested - Irradiated Material

Figure 22. Modified [45]₄ Multiple Cycle Room Temperature Shear Stress-Shear Strain Results
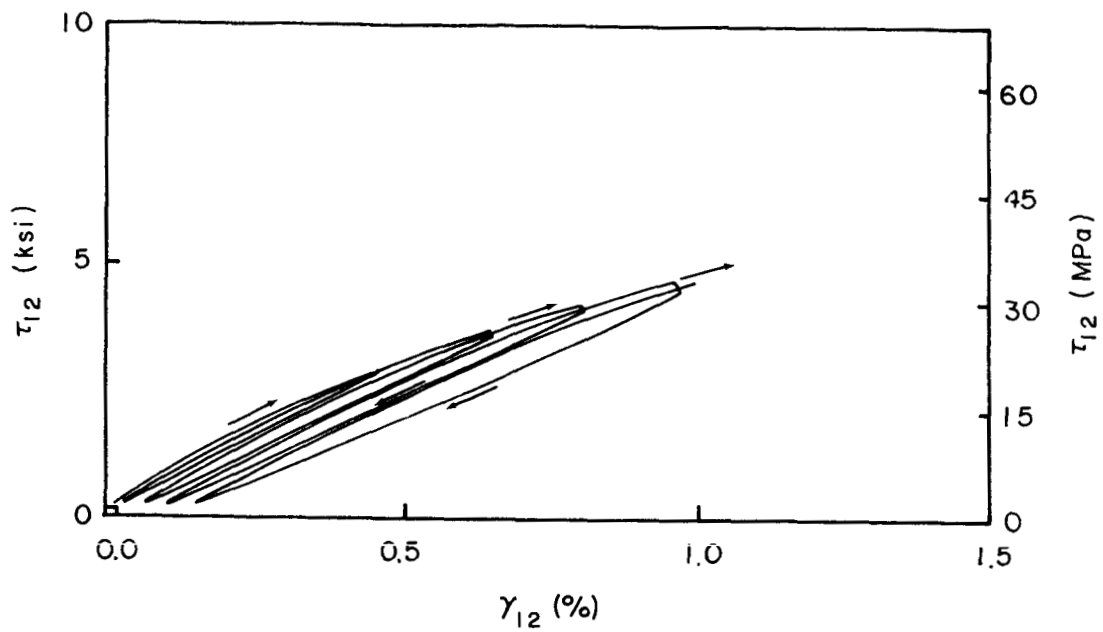
a) Elevated Temperature Tested - Baseline Material
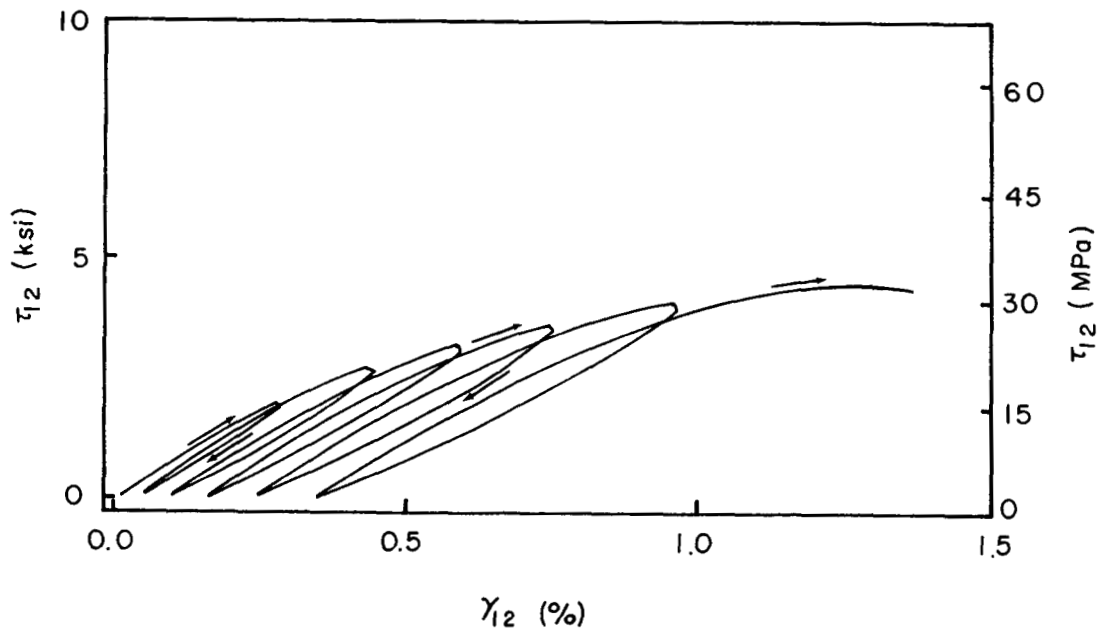
b) Elevated Temperature Tested - Irradiated Material

Figure 23.   Modified [45]₄ Multiple Cycle Elevated Temperature Shear Stress-Shear Strain Results
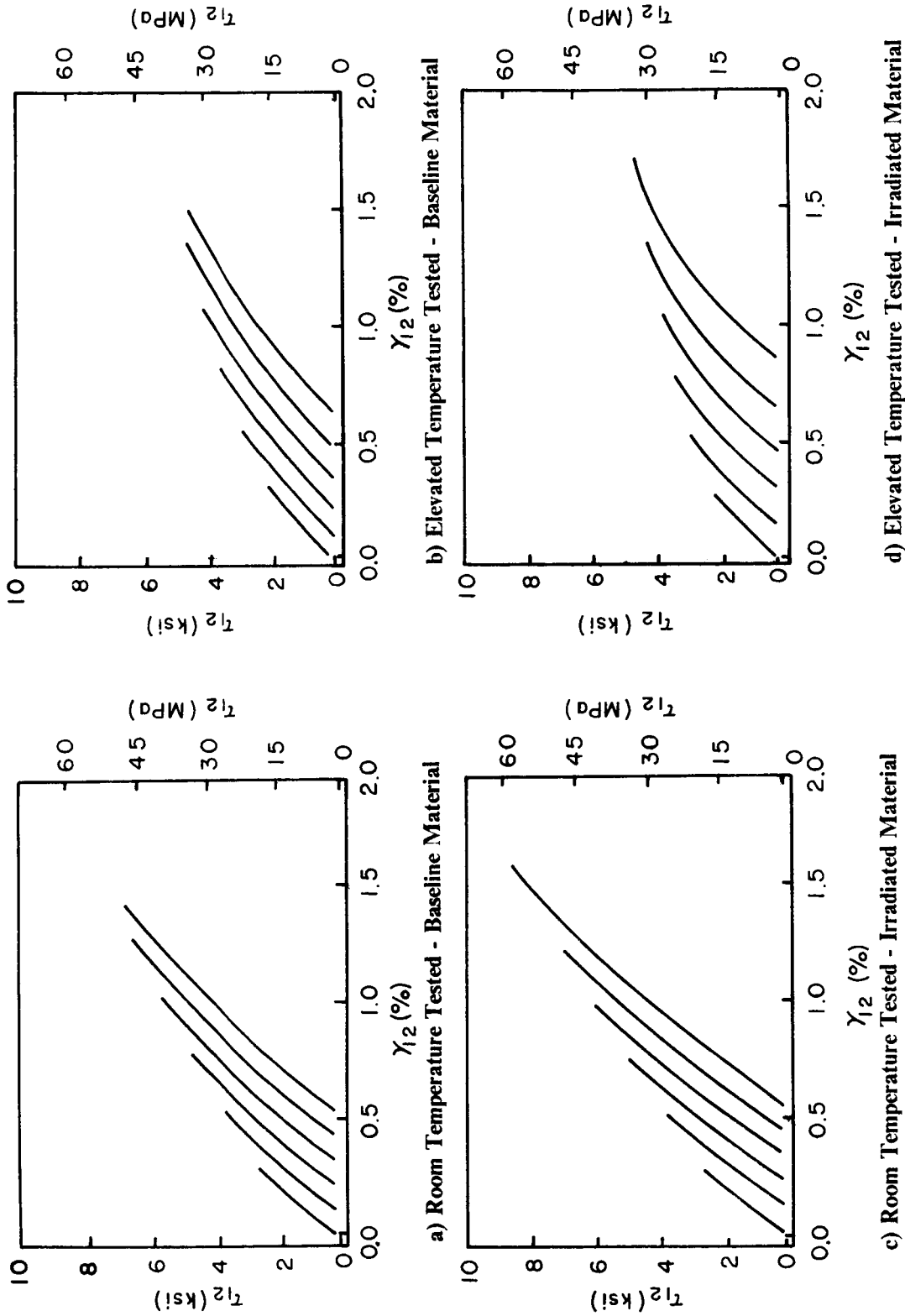
Figure 24. Modified |45|₄ Loadings Only from Multiple Cycle Shear Stress-Shear Strain Results

a) Room Temperature Tested - Baseline Material

b) Elevated Temperature Tested - Baseline Material

c) Room Temperature Tested - Irradiated Material

d) Elevated Temperature Tested - Irradiated Material
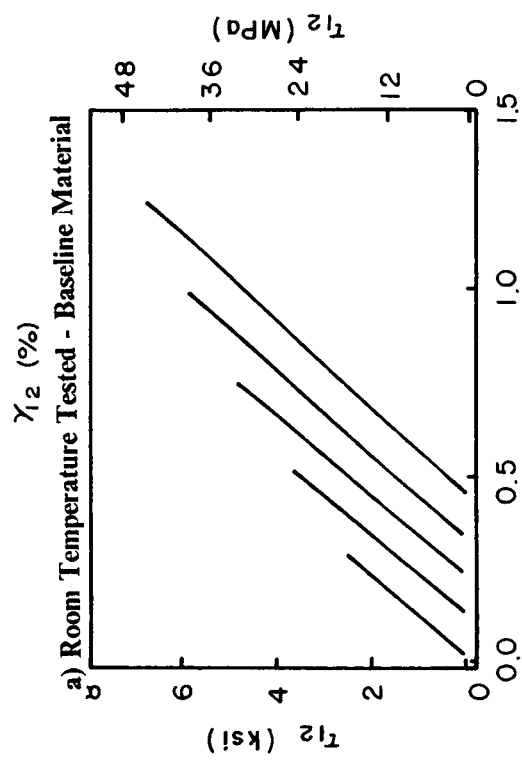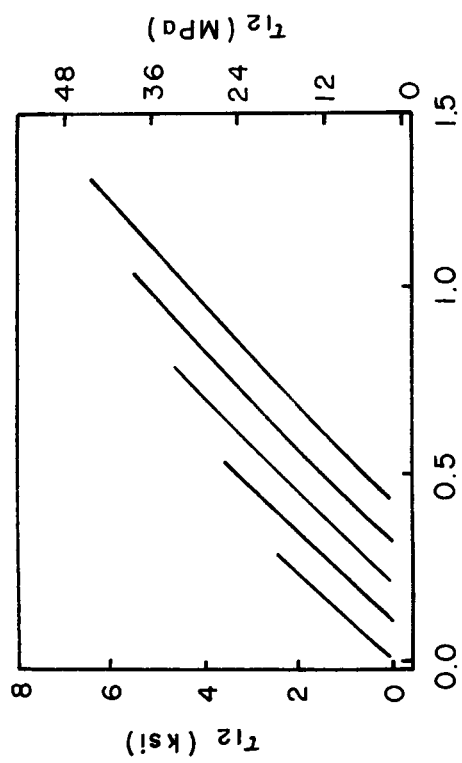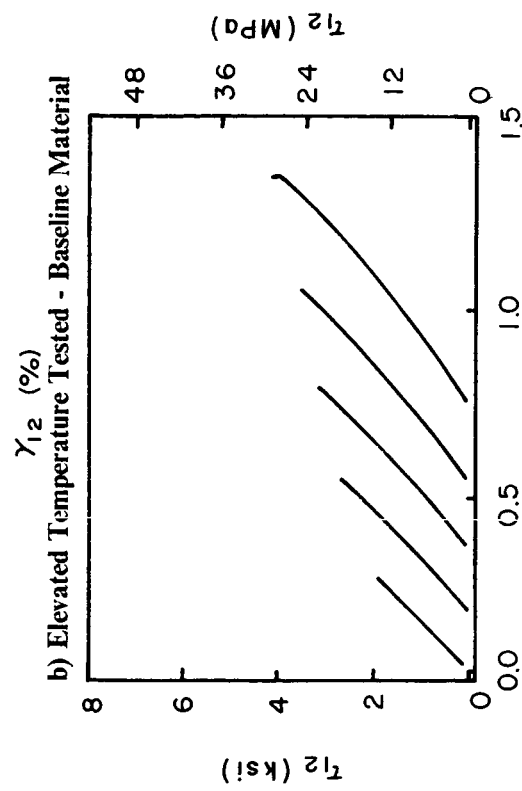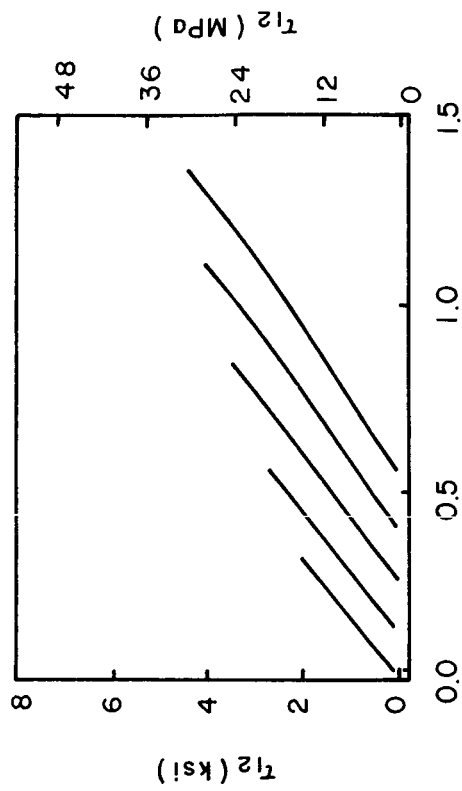
Figure 25. Modified [45]₄ Unloadings Only from Multiple Cycle Shear Stress-Shear Strain Results

a) Room Temperature Tested - Baseline Material

b) Elevated Temperature Tested - Baseline Material

c) Room Temperature Tested - Irradiated Material

d) Elevated Temperature Tested - Irradiated Material

and 19% for both elevated temperature materials). The initial unloading modulus of the first cycle was nearly equal to the initial loading modulus for each material. The effects of damage caused by mechanical cycling and increased loads are seen in the form of decreasing initial unloading moduli. The amount of energy dissipation present is another indication of the extent of material degradation. The elevated temperature tested materials exhibited more dissipation than the room temperature tested materials, with the irradiated cases exhibiting more energy dissipation than the baseline cases. An explanation of the probable causes of degradation is presented in section 3.5.

3.3 Matrix Characterization

Thermomechanical analysis and dynamic-mechanical analysis provide information to determine the effects of irradiation over a wide temperature range on the matrix material. The literature indicates that ionizing radiation causes chain scission and crosslinking in polymers [11], both of which directly affect the glass transition temperature (T_g) of the material. Both the DMA and the TMA provide information about the T_g region and its changes.

3.3.1 DMA

The damping versus temperature data for the $[90]_4$ baseline and irradiated modified material specimens are presented in Fig. 26. These curves show a glass transition temperature, T_g, for the baseline material of 491° F (255° C), and for the irradiated material of 441° F (227° C). In addition to lowering the T_g by 50° F (28° C), irradiation broadens the rubbery range of the material. This range extends for the irradiated material from approximately 175° F (80° C) to 475° F (245° C), whereas
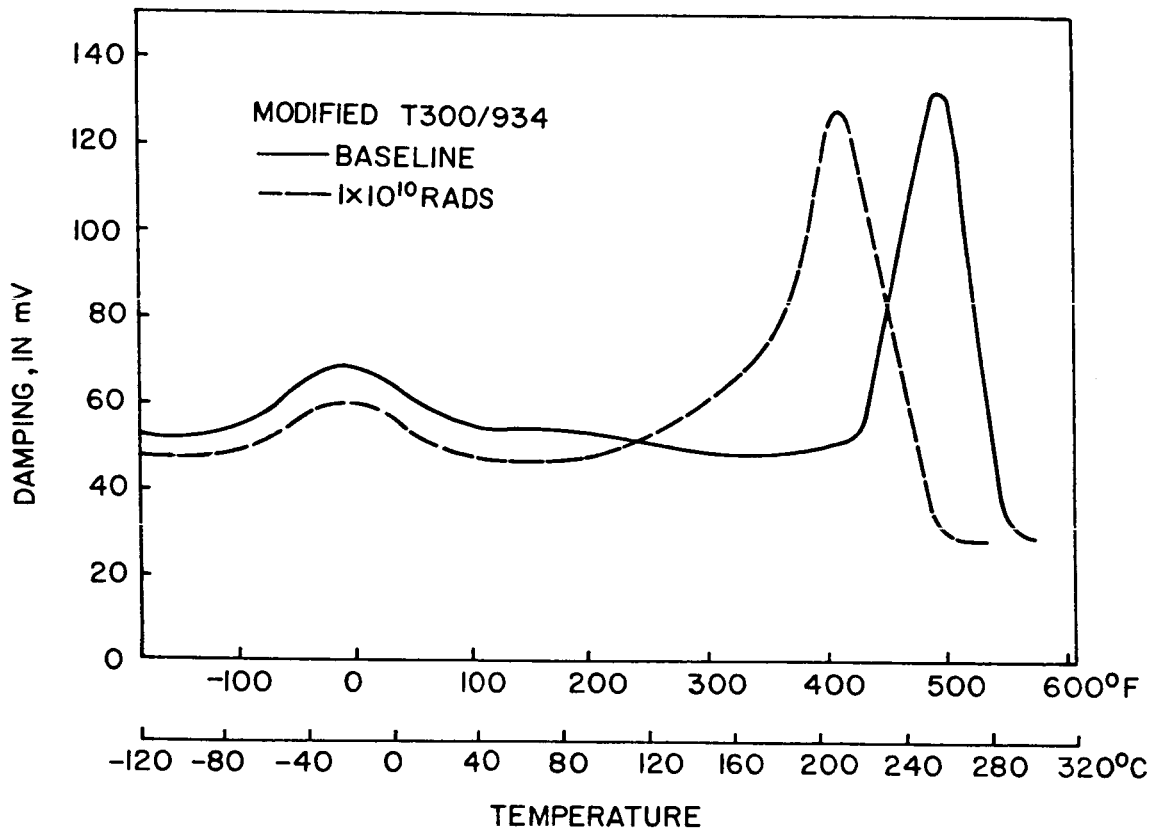
Figure 26.   Damping versus Temperature Modified Material Data

the baseline material has a narrow well-defined peak that extends from 420° F (215° C) to 535° F (280° C). The extended low temperature end of the irradiated material rubbery range indicates the formation of low molecular weight products and the occurrence of chain scissioning. The extended high temperature end of the rubbery range indicates the formation of high molecular weight products. This is due to crosslinking. Chain scission is the predominant event occurring due to irradiation.

Dynamic Young's modulus (tensile storage modulus) as a function of temperature is shown in Fig. 27 for the $[90]_4$ baseline and irradiated modified laminates. These curves show that the modulus of the irradiated material is approximately 10% greater than the baseline material up to 340° F (170° C), but the degradation of the modulus (softening of the material) occurs 72° F (42° C) lower for the irradiated material. These results support the findings from the monotonic tension tests that the irradiated material has a transverse modulus that is greater at room temperature than that of the baseline material. The matrix changes which cause these phenomena are explained in section 3.5.

3.3.2 TMA

The thermomechanical analysis results for the baseline and irradiated modified materials are shown in Fig. 28. The weighted probe begins to penetrate the baseline material at approximately 430° F (220° C). This softening temperature of the material correlates with the temperature at which the DMA damping curve indicates the start of the of the rubbery range for the baseline material (Fig. 26). The irradiated material begins to soften at room temperature and continues softening throughout the temperature range. This correlates to the continuous decrease of modulus exhibited by the DMA tensile storage modulus (Fig. 27). These irradiated material results suggest that there are radiation-generated, low molecular weight products present that plasticize the material, making it softer and more pliable. Around 645° F (340° C), the probe is pushed out of the material as the
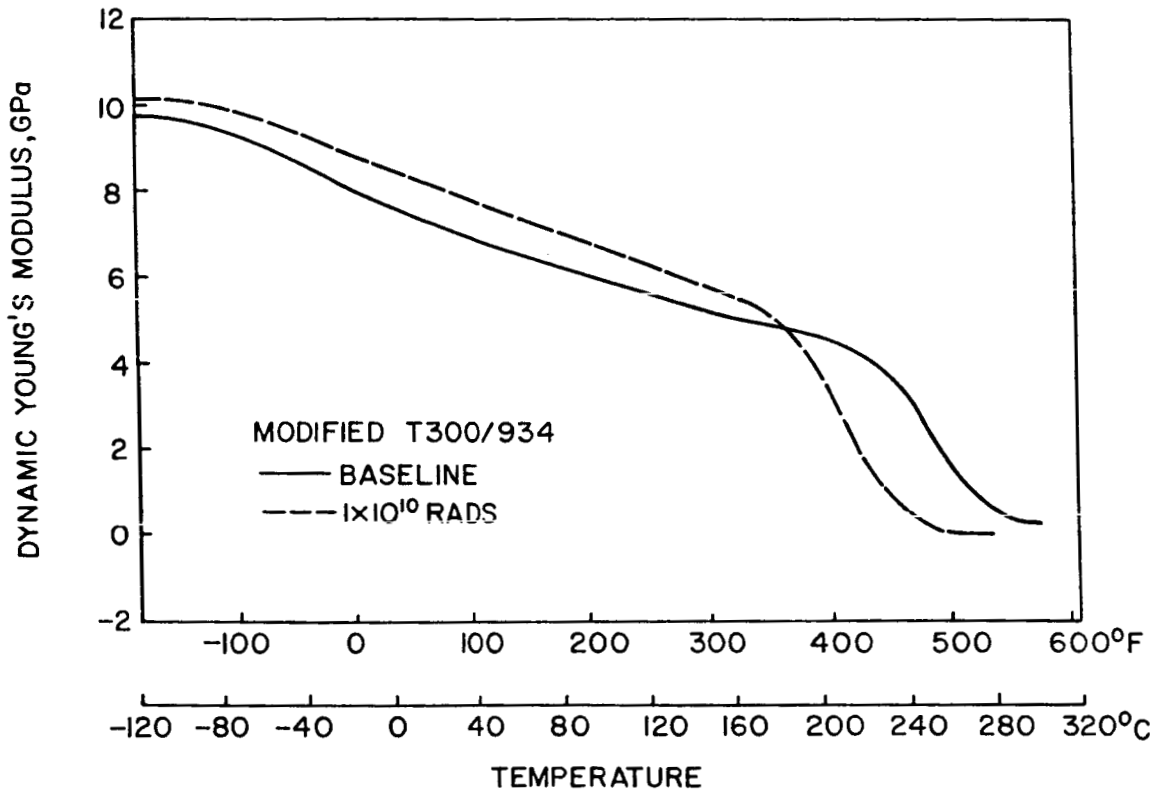
Figure 27. Dynamic Young's Modulus versus Temperature Modified Material Data
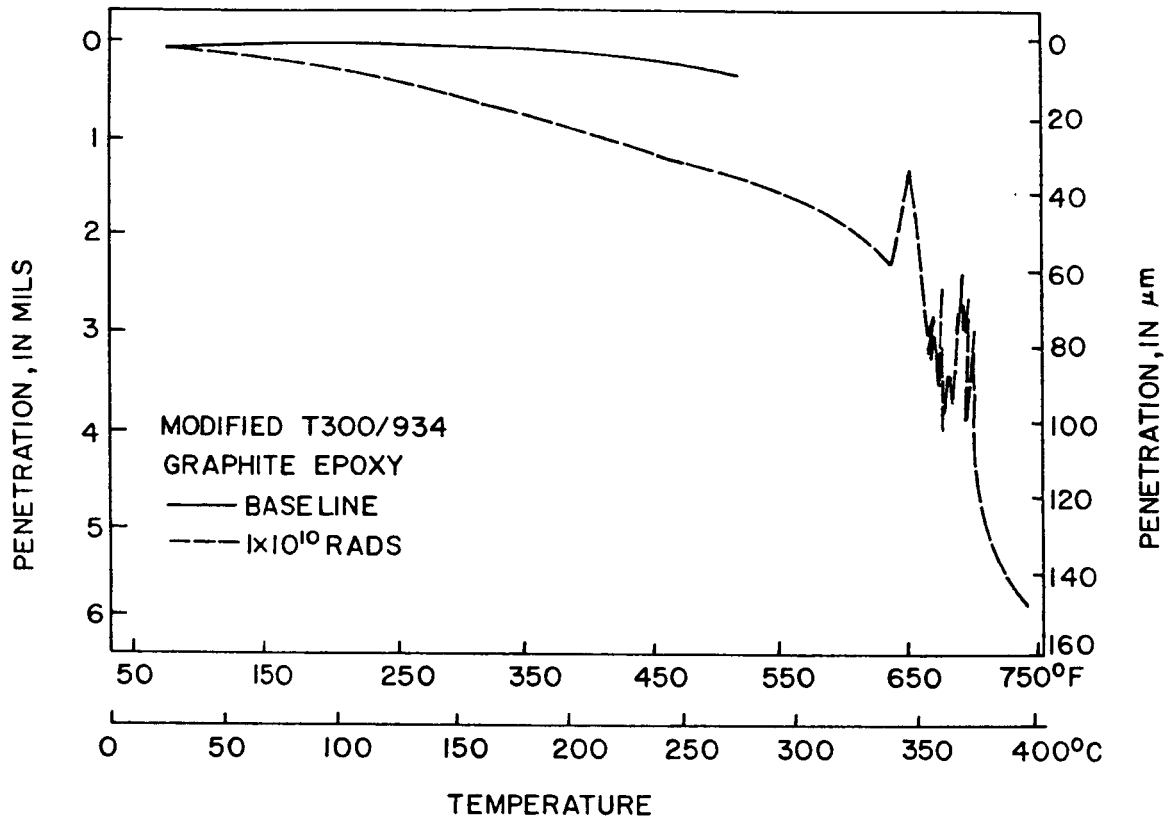
Figure 28. Thermomechanical Analysis Results for the Modified Material

composite begins to expand and delaminate. Knowing that low molecular weight products have a low boiling point, this indicates that the low molecular weight species produced during irradiation are boiling at this temperature forming gas pockets. This trapped gas expands causing delaminations that push the probe from the material.

3.3.3 Photo Methods

Scanning electron micrographs (SEMs) were taken of the failure surface of [45]$_4$ laminates. These photographs are presented at low and high magnifications in Figs. 29 and 30. Approximate magnifications are noted under each picture. The fracture surface of the materials shows that the epoxy is a relatively brittle material in all cases. The only material with a noticeable difference in the matrix fracture surface is the elevated temperature tested irradiated material. From Fig. 30d, an increase in the ductile fracture behavior of the matrix is apparent. The amount of matrix remaining on the fibers of all tests indicates good adhesion between fiber and matrix at the interface. The platelets or "ribbed" effect of the epoxy on the failure surfaces indicates matrix failure and not failure at the fiber-matrix interface bond. A recent study by Funk and Sykes [12] supports the idea that failure does not occur at the fiber-matrix interface. Plasticization of the epoxy due to irradiation combined with high temperature, and material failure of these [45]$_4$ laminates due to the matrix material correlates with the behavior exhibited in the [45]$_4$ tension tests (Figs. 14 and 15). The increased plasticization and ductility of the irradiated material at elevated temperature is expected as these tests were conducted within the irradiated material's rubbery range (Fig. 26).

Failed [45]$_4$ room temperature laminates were X-rayed to detect any microcracking that might be present. These specimens were exposed to a zinc oxide penetrate before X-raying. None of the specimens showed damage. This could possibly be because either there was no damage in the material or because damage can only be detected while the material is under a tensile load.

b) Elevated Temperature Tested - Baseline Material - 387.5X

a) Room Temperature Tested - Baseline Material - 300X

d) Elevated Temperature Tested - Irradiated Material - 450X

c) Room Temperature Tested - Irradiated Material - 325X

Figure 29.   Scanning Electron Micrographs of [45]₄ Fracture Surfaces, Low Magnifications

Results and Discussion

a) Room Temperature Tested - Baseline Material - 3000X

b) Elevated Temperature Tested - Baseline Material - 3875X

c) Room Temperature Tested - Irradiated Material - 3250X

d) Elevated Temperature Tested - Irradiated Material - 4500X

Figure 30. Scanning Electron Micrographs of [45]₄ Fracture Surfaces, High Magnifications

3.4 Graphite Fiber Tests

The elastic modulus, determined from the load-time graph and the time-displacement relationship, and the tensile strength results for baseline and irradiated graphite fiber tension tests are presented in Table 4. Tabulated data are presented in Appendix B. These results show no significant degradation of elastic modulus nor ultimate strength due to irradiation. This conclusion compliments the assumptions of Milkovich et al. [2], and the findings of Kent, Wolf, Memory, Fornes and Gilbert [13] , and Haskins [4].

3.5 Matrix Microstructure Changes

The material behavior exhibited in the above results is due to irradiation and/or temperature. The changes are attributed to the epoxy material as the graphite fibers are unaffected by the elevated temperature in the test range and radiation dosages of 1×10^{10} rads.

The cured epoxy can be imagined as having a 3-D structure, where the chains are interconnected by crosslinks. Elevated temperatures and radiation exposure were found to influence the behavior of the material. Irradiation breaks some of the bonds that link the polymer chains together [14, 15]. This permits stretching in the material, and chains to slide relative to one another. At temperatures near the T_g, the low molecular weight products formed during irradiation plasticize the material. This accounts for the softening of the irradiated material at a lower temperature than the baseline material.

Table 4. Fiber Test Results

PROPERTIES		RADIATION DOSAGE	
		NON-IRRADIATED	1×10^{10} RADS
ELASTIC MODULUS (MSI)	AVERAGE	34.8	33.5
	STANDARD DEVIATION	1.29	1.24
	95% CONFIDENCE INTERVAL	32.3 - 37.3	31.1 - 35.9
TENSILE STRENGTH (KSI)	AVERAGE	547	517
	STANDARD DEVIATION	99.3	78.7
	95% CONFIDENCE INTERVAL	352 - 742	363 - 671

For the $[0]_4$ tests, elevated temperatures and irradiation degrade the epoxy, reducing residual stresses between fibers and matrix. Reduced residual stresses result in straighter fibers and more efficient load transfer in high stress concentration regions, such as fiber breaks [16].

For increasing off-axis orientations, the relationship between the room temperature tested baseline and irradiated materials changes (Figs. 10, 12, 14 and 16). For both the $[0]_4$ and $[10]_4$ laminates, the room temperature tested baseline and irradiated materials (Figs. 10, 12 and 13), exhibit equal elastic moduli, but in all of the $[45]_4$ tests (Figs. 12 and 16), the irradiated material exhibits a higher initial modulus. Increased non-linearity of the irradiated material, which causes this curve to cross over the baseline curve, is also exhibited. The higher strain at failure is due to the increased ductility of the irradiated material. In the matrix dominated $[90]_4$ tests, the irradiated material exhibits a higher elastic moduli than the baseline material at room temperature. The effect of radiation on the room temperature tested material is possibly due to the low molecular weight products which are formed from the broken bonds in the matrix network structure during irradiation. These products are trapped within the network, filling the free volume and partially restricting movement of the molecular chains. This action causes the material to appear glassy, accounting for the higher modulus both for these laminates and the $[45]_4$ laminates at low stresses. At higher stresses the polymer chains begin to slide relative to each other. This allows the material to stretch and exhibit increased ductility. At elevated temperatures these low molecular weight products in the irradiated material vaporize and act as plasticizers to soften the material. This causes a decrease in ultimate stress and an increase in ultimate strain (i.e. increased ductility).

From the cyclic tests (Figs. 17-21) it is evident that irradiation of the material causes a greater increase of energy dissipation than exposure to elevated temperatures. The dissipation of the irradiated material is probably due to plasticization as microcracking was ruled out by means of the X-ray photo results. The broken bonds in the irradiated material allow greater molecular chain movement when a stress is applied. At elevated temperatures the effect is more pronounced, thus having a greater effect on material properties. During unloading the irradiated material does not

behave elastically, accounting for the increased permanent strain. A study has not been conducted to characterize the possible time dependent behavior of these phenomena.

From the DMA, the expansion of the irradiated material rubbery range (Fig. 26) suggests that irradiation causes both chain scission and crosslinking in the epoxy network. The irradiation produced low molecular weight products provide a wide distribution of molecular species which can absorb energy over an extended temperature range. This causes the rubbery range expansion. The lowered T_g and broader rubbery range affect elevated temperature properties of the material and suggest a degradation of the 3-D epoxy network.

The TMA results show that the irradiated material begins to soften at room temperature and at elevated temperature the irradiation produced by-products boil and vaporize, causing delaminations in the composite material.

3.6   Comparison of T300/934 Materials

The effects of chemically modifying the Fiberite 934 epoxy in an attempt to produce a more radiation resistant material shall be discussed here by comparing the modified system with the standard T300/934 graphite-epoxy composite investigated in reference [2].

A difference in the fabrication method of the panels for each material should be noted. The commercially available T300/934 panels were made using established techniques. The modified material was fabricated using processes which may or may not have been optimum for the experimental material system. Many characteristics of this one-of-a-kind material, such as panel thickness and fiber volume fraction, were found to be non-uniform. Comparisons of these properties with the standard material properties are presented in Table 1.

Mechanical Properties Comparison

Comparisons of in-plane mechanical properties with those reported by Milkovich et al. [2] are listed below. Differences were slight in most cases, and trends in both material systems were most often similar.

- E_1: In general, the elastic modulus of the modified material is higher, with a noticeable increase in modulus from the room temperature tests to the elevated temperature tests. The standard material has no significant change in modulus for the different cases.

- X_T: No conclusive results can be drawn due to incomplete failure data of the $[0]_4$ laminates. Trends, though, indicate that these materials exhibited roughly the same longitudinal tensile strength, and possibly higher strength for the modified elevated temperature tested irradiated material.

- v_{12}: Poisson's ratio for the modified material is fairly constant, where that of the standard material has a decreased v_{12} for the room temperature irradiated material and an increased v_{12} for the elevated irradiated material.

- S: A slight increase in ultimate shear stress at failure for the room temperature tested modified materials is noted. Elevated temperature tests for the modified and standard materials are consistent.

- G_{12}: Even though this value was calculated using different methods for the modified and standard materials, the values are essentially equal.

- E_2: In general, the modified material specimens have transverse elastic moduli equivalent to that of the standard material specimens. The exception is for the irradiated elevated temperature tested modified material. This case shows a significantly lower modulus.

- Y_T: Ultimate transverse stress values compare in the same fashion as E_2.

Cycled Tests

Cyclic tests for the standard T300/934 material were conducted. Typical results in terms of axial stress versus axial strain are presented in Figs. 31-33 for the $[10]_4$, $[45]_4$, $[90]_4$ laminates, respectively. Results in terms of shear stress versus shear strain for the $[10]_4$ and $[45]_4$ laminates are presented in Figs. 34 and 35. The tests of the baseline material often include two or more cycles. The irradiated material was cycled only once.

The $[10]_4$ and $[45]_4$ baseline and irradiated materials show significant energy dissipation in the elevated temperature tests. The $[90]_4$ material exhibits energy dissipation only for the elevated temperature tested irradiated material. The major difference between the standard material and the modified material is that the irradiated modified material room temperature tests show a significant amount of energy dissipation, whereas the standard material does not. Trends exhibited in both materials are that the elevated temperature irradiated specimens do not reload through the turning point of the previous cycle and that they exhibit more permanent strain than the elevated baseline specimens.

Dynamic-mechanical analysis for the standard T300/934 is presented in Fig. 36 as damping versus temperature and in Fig. 37 as Dynamic Young's modulus versus temperature. This data shows that the T_g for the baseline material is 455° F (235° C) and for the irradiated material is 385° F (196° C). The T_g of the standard material is lowered 70° F (39° C) by irradiation. Comparing the baseline modified and standard materials, the T_g is found to be 36° F (20° C) higher but the rubbery range is slightly broader for the modified material. For the irradiated specimens, the modification of the material has increased the T_g by 56° F (31° C), and the width of the peak has remained essentially the same. Dynamic Young's modulus shows that the modified material exhibits softening temperatures that are slightly greater than those of the standard material (Figs. 27 and 37).

Thermomechanical analysis of the two materials indicates that the modified material begins to soften at much higher temperatures than the standard material, and though the irradiated modified material softens at 350° F (150° C), vaporization and delamination do not occur at this temperature
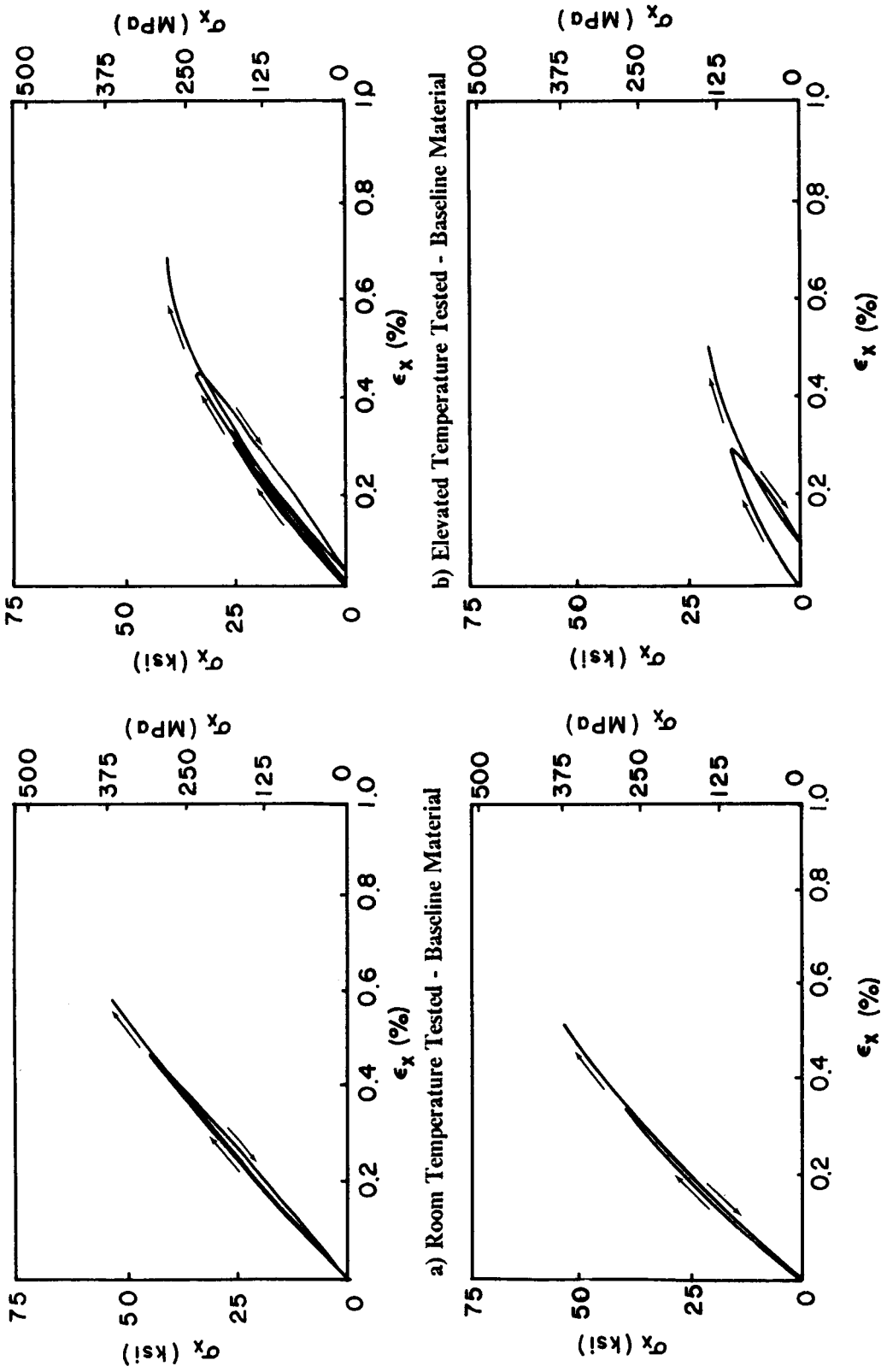
Figure 31. Standard |10|₄ Cyclic Tension Stress-Strain Results

a) Room Temperature Tested - Baseline Material

b) Elevated Temperature Tested - Baseline Material

c) Room Temperature Tested - Irradiated Material

d) Elevated Temperature Tested - Irradiated Material

b) Elevated Temperature Tested - Baseline Material

d) Elevated Temperature Tested - Irradiated Material

a) Room Temperature Tested - Baseline Material

c) Room Temperature Tested - Irradiated Material

Figure 32.   Standard [45]₄ Cyclic Tension Stress-Strain Results
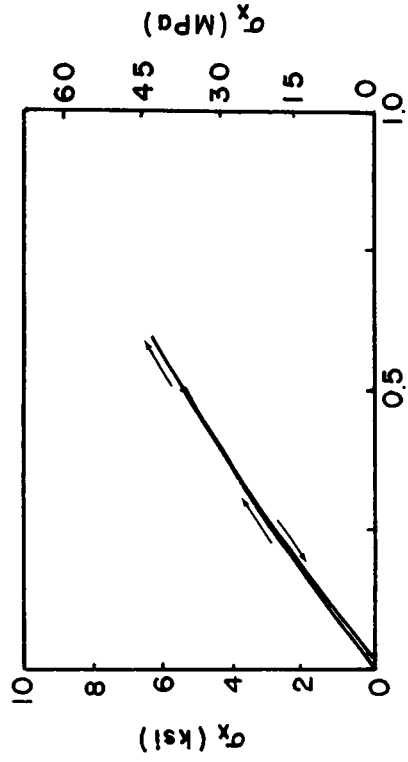
a) Room Temperature Tested - Baseline Material
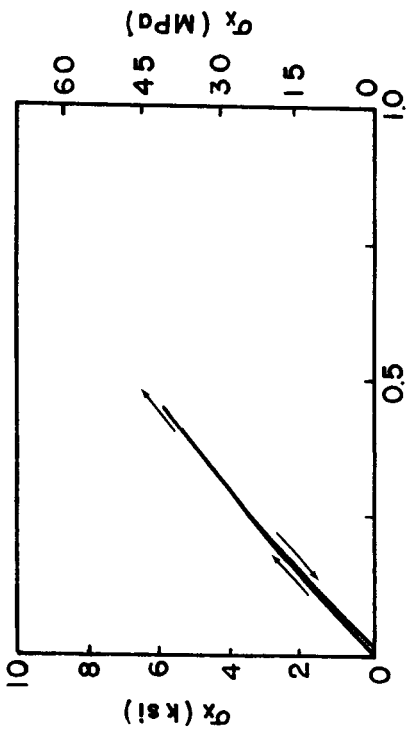
b) Elevated Temperature Tested - Baseline Material
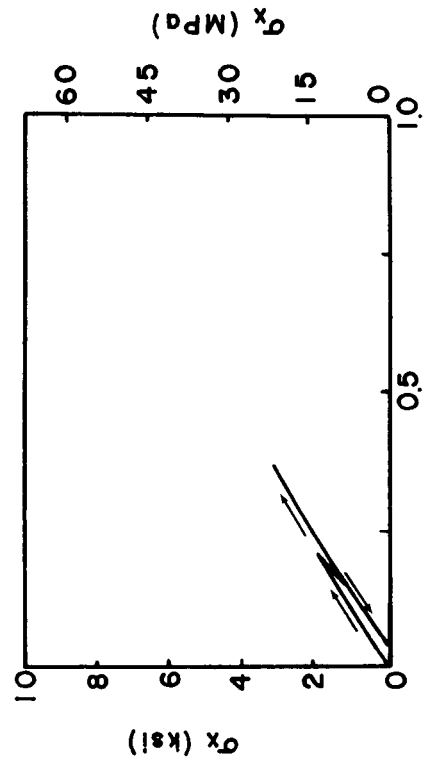
c) Elevated Temperature Tested - Irradiated Material

Figure 33.   Standard [90]₄ Cyclic Tension Stress-Strain Results
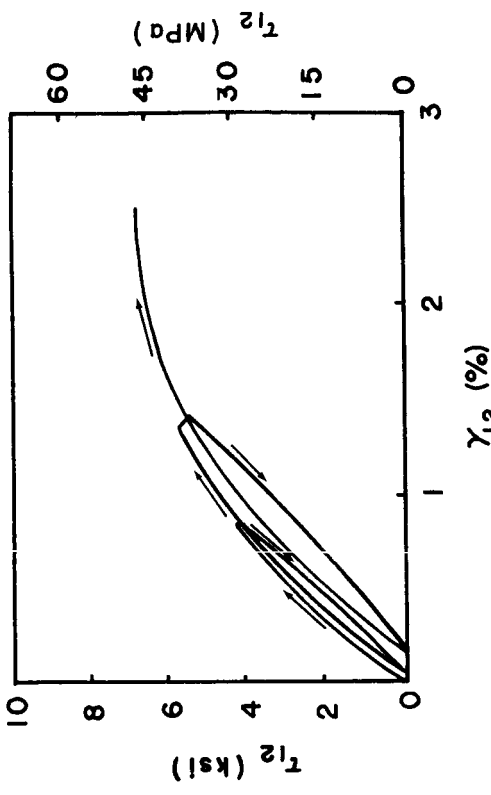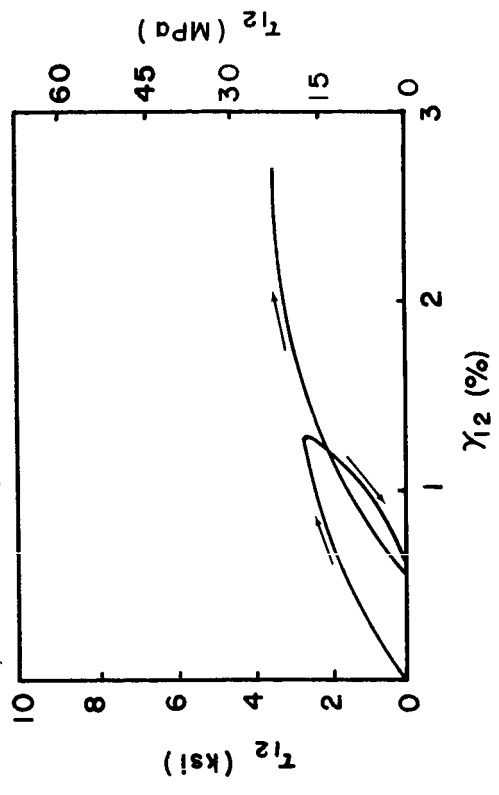
b) Elevated Temperature Tested - Baseline Material

d) Elevated Temperature Tested - Irradiated Material
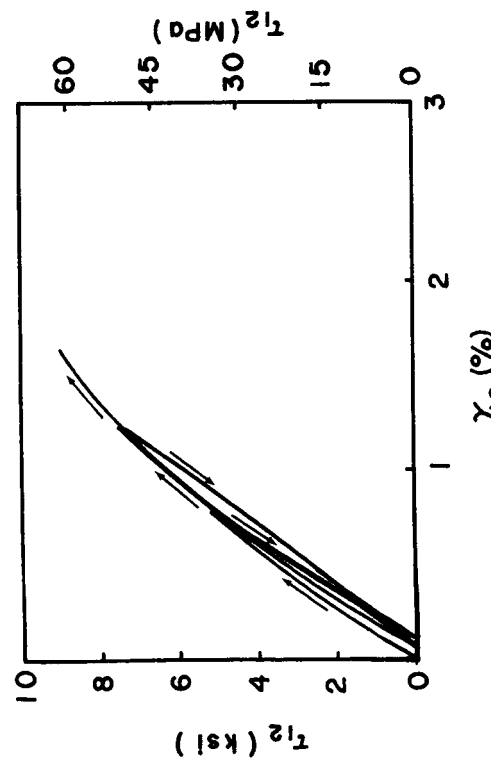
a) Room Temperature Tested - Baseline Material
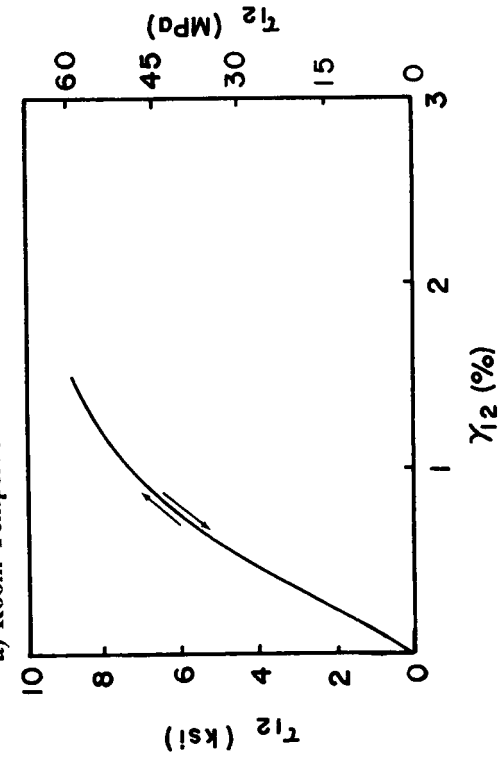
c) Room Temperature Tested - Irradiated Material

Figure 34. Standard |10|₄ Cyclic Shear Stress-Shear Strain Results
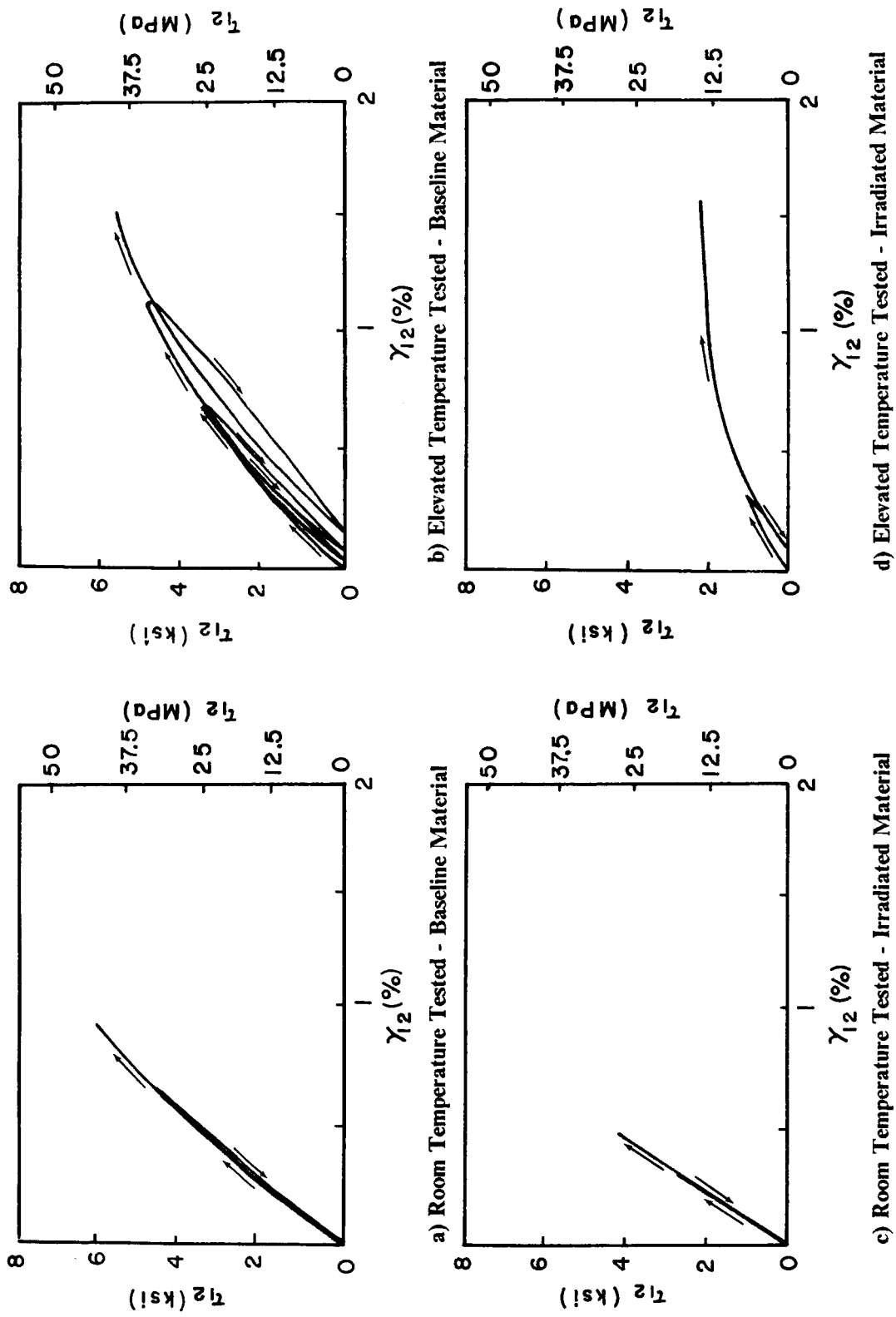
Figure 35.   Standard [45]₄ Cyclic Shear Stress-Shear Strain Results

a) Room Temperature Tested - Baseline Material

b) Elevated Temperature Tested - Baseline Material

c) Room Temperature Tested - Irradiated Material

d) Elevated Temperature Tested - Irradiated Material
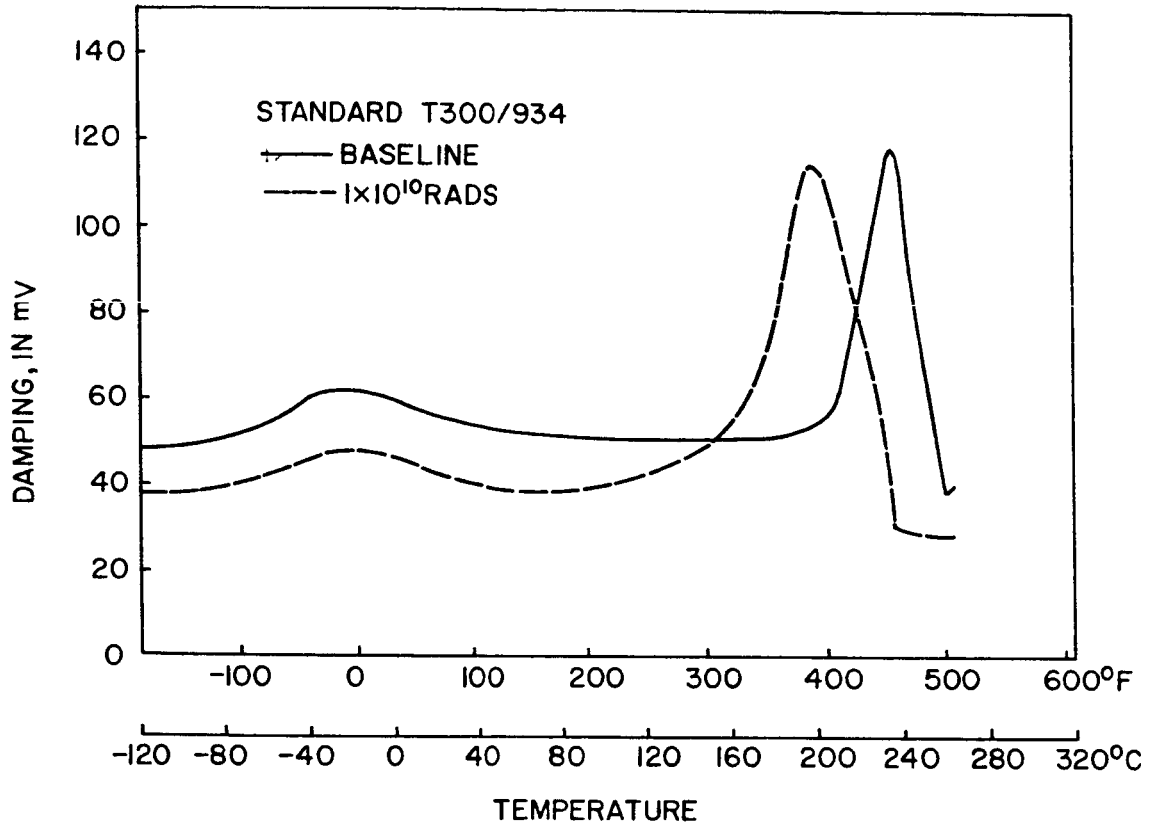
Figure 36. Damping versus Temperature Standard Material Data
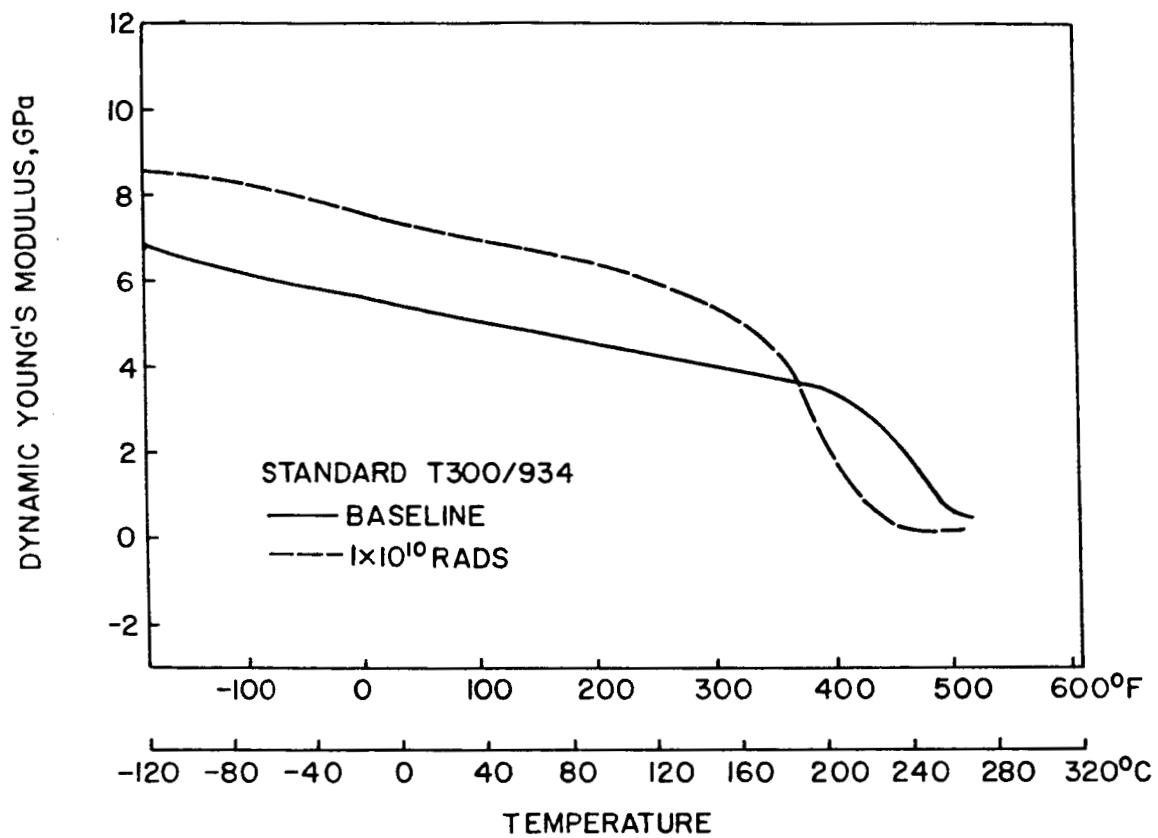
Figure 37. Dynamic Young's Modulus versus Temperature Standard Material Data

as they do for the standard material. Delamination of the modified material occurs at temperatures of 660° F (350° C) and higher.

4.0 Conclusions

A summary of the results of this study into the effects of the GEO environment on a chemically modified graphite-epoxy composite material is presented below. Note that a graphite-epoxy structure in actual space conditions during a 30 year service life may be influenced to a different degree than observed under these accelerated test conditions.

1. A radiation dosage of 1×10^{10} rads affects the mechanical behavior of a graphite-epoxy composite material by altering the chemical structure of the epoxy matrix.

   - Chain scission occurs during irradiation. This event coupled with elevated temperatures softens the material and increases ductility. These degradation effects can also be observed in the lowered glass transition temperature of the irradiated material.

   - The low molecular weight products generated during irradiation fill the free volume at room temperature and vaporize at elevated temperatures. These by-products are also responsible for expanding the rubbery range of the irradiated material.

   - The low molecular weight products produced during irradiation effectively stiffen the composite material at room temperature, but cause severe degradation at 250° F (121° C) and blistering and delamination at higher temperatures.

- Strength appears to be equally affected by irradiation and elevated temperatures, but a combination of the two effects causes a much further reduction in the material's ultimate stress, especially in the matrix dominated orientations.

- Radiation does not affect the strength or stiffness of graphite fibers.

2. The irradiated material exhibits increased energy dissipation as compared to the baseline material. This suggests the irraadiated material has a non-continuous epoxy network structure due to broken bonds. The continuous structure of the baseline material transfers energy more easily, thereby exhibiting much less energy dissipation in the cycled tests.

3. The chemical modification of the material did not significantly aid in producing a more radiation resistant material. The modified material exhibits slightly increased glass transition temperatures, but also exhibits increased amounts of energy dissipation due to irradiation. The modified material appears to behave in a more time-dependent manner than the standard material.

Recommendations for Further Study

- Characterize the space environment effects on the time dependent behavior of the graphite-epoxy material.

- Conduct an investigation as to the effects of radiation on the compressive properties of the material.

- Study the radiation effects on the bulk properties of standard and modified epoxies to further examine the chemical structure changes that occur.

5.0 References

1. Tenney, D. R., Sykes, G. F. and Bowles, D. E., "Composite Materials for Space Structures,"
    presented at the Third European Symposium on Spacecraft Materials in Space Environment,
    Noordwijk, The Netherlands, October 1-4, 1985.

2. Milkovich, S. M., Herakovich, C. T. and Sykes, G. F., "Space Radiation Effects on
    Graphite-Epoxy Composite Materials," VPI-E-84-20, Virginia Polytechnic Institute and State
    University, 1984.

3. Sykes, G. F., Milkovich, S. M. and Herakovich, C. T., "Simulated Space Radiation Effects on
    a Graphite Epoxy Composite," *Polymeric Materials Science and Engineering* , Proceedings of
    the ACS Division of Polymeric Materials: Science and Engineering, Volume 52, American
    Chemical Society, 1985, pp.598-603.

4. Haskins, J. F., "Advanced Composite Design Data for Spacecraft Structural Applications,"
    presented at the 12th National SAMPE Technical Conference, Seattle, Washinton, October
    7-9, 1980.

5. Pindera, M. J. and Herakovich, C. T., "An Endochronic Theory for Transversely Isotropic Fibrous Composites," VPI-E-81-27, Virginia Polytechnic Institute and State University, October 1981.

6. Nielsen, L. E., *Mechanical Properties of Polymers*, Reinhold Publishing Corporation, New York, New York, 1967.

7. Hyer, M. W., Herakovich, C. T., Milkovich, S. M. and Short, J. S., "Temperature Dependence of Mechanical and Thermal Expansion Properties of T300/5208 Graphite/Epoxy," *Composites*, Volume 14, Number 3, July 1983, pp. 276-280.

8. Tsai, S. W., *Composites Design 1986*, Think Composites, Dayton, Ohio, 1986.

9. Pindera, M. J. and Herakovich, C. T., "Shear Characterization of Unidirectional Composites with Off-Axis Tension Test," *Experimental Mechanics*, Volume 26, Number 1, March 1986, pp. 103-111.

10. Nielsen, L. E., *Mechanical Properties of Polymers and Composites*, Marcel Dekker, Inc., New York, 1974.

11. Moore, G. R. and Kline, D. E., *Properties and Processing of Polymers for Engineers*, Prentice-Hall, Englewood Cliffs, New Jersey, 1984.

12. Funk, J. G. and Sykes, G. F., "The Effects of Radiation on the Interlaminar Fracture Toughness," *Journal of Composite Technology and Research*, to be published Fall 1986.

13. Kent, M., Wolf, K., Memory, J. D., Fornes, R. E. and Gilbert, R. D., *Carbon*, Volume 22, Number 1, 1984, pp. 103-104.

14. Giori, C., Yamauchi, T., Rajan, K. and Mell, R., "Mechanisms of Degradation of Graphite Composites in Simulated Space Environment," presented at the AIAA 21st Aerospace Sciences Meeting, Reno, Nevada, January 10-13, 1983.

15. Mauri, R. E. and Crossman, F. W., "Space Radiation Effects on Structural Composites," presented at the AIAA 21st Aerospace Sciences Meeting, Reno, Nevada, January 10-13, 1983.

16. Milkovich, S. M. and Herakovich, C. T., "Temperature Dependence of Elastic and Strength Properties of T300/5208 Graphite-Epoxy," VPI-E-83-9, Virginia Polytechnic Institute and State University, April 1984.

Appendix A.

Shear Modulus, G_{12}, Formulation

From the rosette strain gages applied to the $[10]_4$ and $[45]_4$ specimens, the longitudinal, transverse and 45° strains were measured. Having this data and the corresponding axial stress data, the shear stress, τ_{12}, and shear strain, γ_{12}, are calculated using the following formulation:
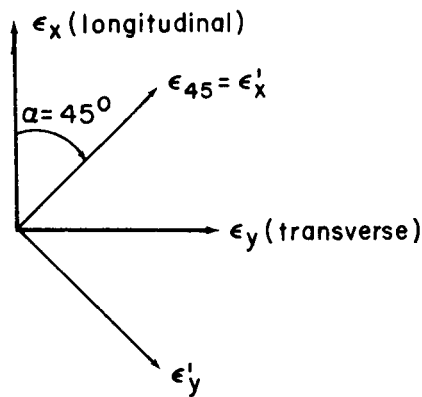
To find ε_{45} (ε'_x) in terms of ε_x, ε_y and ε_{xy}, the strain transformation through an angle of 45° is used.

$$\begin{Bmatrix} \varepsilon'_x \\ \varepsilon'_y \\ \dfrac{\gamma'_{xy}}{2} \end{Bmatrix} = \begin{bmatrix} \cos^2\alpha & \cos^2\alpha & 2\cos\alpha\sin\alpha \\ \sin^2\alpha & \cos^2\alpha & -2\cos\alpha\sin\alpha \\ -\cos\alpha\sin\alpha & \cos\alpha\sin\alpha & \cos^2\alpha - \sin^2\alpha \end{bmatrix} \begin{Bmatrix} \varepsilon_x \\ \varepsilon_y \\ \dfrac{\gamma_{xy}}{2} \end{Bmatrix}$$

$$\varepsilon'_x = \cos^2\alpha\varepsilon_x + \sin^2\alpha\varepsilon_y + \sin\alpha\cos\alpha\gamma_{xy}$$

Or conversely, knowing $\alpha = 45°$:

$$\gamma_{xy} = -(\varepsilon_x + \varepsilon_y) + 2\varepsilon_{45}$$

Having ε_x, ε_y and γ_{xy}, the strain transformation equation can be employed again to find the shear strain, γ_{12}. The angle, θ, is the material orientation measured clockwise from the axial direction.

$$\left\{ \begin{array}{c} \varepsilon_1 \\ \varepsilon_2 \\ \dfrac{\gamma_{12}}{2} \end{array} \right\} = \left[\begin{array}{ccc} \cos^2\theta & \sin^2\theta & 2\cos\theta\sin\theta \\ \sin^2\theta & \cos^2\theta & -2\cos\theta\sin\theta \\ -\cos\theta\sin\theta & \cos\theta\sin\theta & \cos^2\theta - \sin^2\theta \end{array} \right] \left\{ \begin{array}{c} \varepsilon_x \\ \varepsilon_y \\ \dfrac{\gamma_{xy}}{2} \end{array} \right\}$$

$$\gamma_{12} = 2\cos\theta\sin\theta(\varepsilon_y - \varepsilon_x) + (\cos^2\theta - \sin^2\theta)\gamma_{xy}$$

or,

$$\gamma_{12} = 2\cos\theta\sin\theta(\varepsilon_y - \varepsilon_x) + (\cos^2\theta - \sin^2\theta)(-\varepsilon_x - \varepsilon_y + 2\varepsilon_{45})$$

Rearranging in terms of measured strains,

$$\gamma_{12} = \varepsilon_x(\sin^2\theta - \cos^2\theta - 2\sin\theta\cos\theta) + \varepsilon_y(\sin^2\theta - \cos^2\theta + 2\sin\theta\cos\theta) + 2\varepsilon_{45}(\cos^2\theta - \sin^2\theta)$$

For the shear stress, the stress transformation equation is used.

$$\left\{ \begin{array}{c} \sigma_1 \\ \sigma_2 \\ \tau_{12} \end{array} \right\} = \left[\begin{array}{ccc} \cos^2\theta & \sin^2\theta & 2\cos\theta\sin\theta \\ \sin^2\theta & \cos^2\theta & -2\cos\theta\sin\theta \\ -\cos\theta\sin\theta & \cos\theta\sin\theta & \cos^2\theta - \sin^2\theta \end{array} \right] \left\{ \begin{array}{c} \sigma_x \\ \sigma_y \\ \tau_{x'} \end{array} \right\}$$

Assuming $\sigma_y = \tau_{xy} = 0$, we have:

$$\tau_{12} = -\cos\theta\sin\theta\,\sigma_x$$

Knowing

$$G_{12} = \frac{\tau_{12}}{\gamma_{12}},$$

$|\gamma_{12}|$ versus $|\tau_{12}|$ is plotted and a least square's fit is used to calculate the initial slope, G_{12}.

Formulation of Correction for Gage Misalignment

The misalignment angle, β, is the angle between the coupon axis (along which there are the true strains denoted by ε_{x_t}, ε_{y_t} and ε_{45_t}) and the gage axis (with measured strains ε_{x_m}, ε_{y_m} and ε_{45_m}).
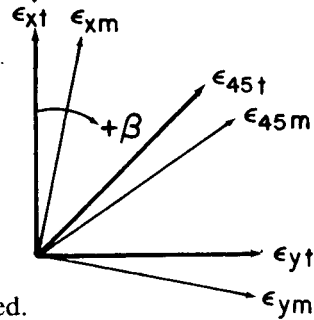
The strain transformation is used.

$$
\left\{ \begin{array}{c} \varepsilon_{x_t} \\ \varepsilon_{y_t} \\ \dfrac{\gamma_{xy_t}}{2} \end{array} \right\} = \left[\begin{array}{ccc} \cos^2\beta & \sin^2\beta & -2\cos\beta\sin\beta \\ \sin^2\beta & \cos^2\beta & 2\cos\beta\sin\beta \\ \cos\beta\sin\beta & -\cos\beta\sin\beta & \cos^2\beta - \sin^2\beta \end{array} \right] \left\{ \begin{array}{c} \varepsilon_{x_m} \\ \varepsilon_{y_m} \\ \dfrac{\gamma_{xy_m}}{2} \end{array} \right\}
$$

From the previous formulation:

$$
\gamma_{xy} = 2\varepsilon_{xy} = -\varepsilon_{x_m} - \varepsilon_{y_m} + 2\varepsilon_{45_m}
$$

Therefore,

$$
\varepsilon_{x_t} = \varepsilon_{x_m}(\cos^2\beta + \cos\beta\sin\beta) + \varepsilon_{y_m}(\sin^2\beta + \cos\beta\sin\beta) - 2\varepsilon_{45_m}\cos\beta\sin\beta
$$

$$
\varepsilon_{y_t} = \varepsilon_{x_m}(\sin^2\beta - \cos\beta\sin\beta) + \varepsilon_{y_m}(\cos^2\beta - \cos\beta\sin\beta) + 2\varepsilon_{45_m}\cos\beta\sin\beta
$$

$$\frac{\gamma_{x_{yt}}}{2} = \varepsilon_{x_m}(2\cos\beta\sin\beta + \sin^2\beta - \cos^2\beta) + \varepsilon_{y_m}(-2\cos\beta\sin\beta + \sin^2\beta - \cos^2\beta)$$

$$+ 2\varepsilon_{45_m}(\cos^2\beta - \sin^2\beta)$$

Table B.1
Individual Test Data for the Modified [0]₄ Laminates

Material/Temp		E_1 (msi)	ν_{12}	X_T (ksi)	$\varepsilon_{1_{ult}}$ (%)	$E_{1_{final}}$ (ksi)	$\sigma_{prop\,limit}$ (ksi)
Baseline (Non-Irradiated)	Room Temp. (75°F) (24°C)	21.45 21.38 20.50 21.25 20.52 21.02	0.3317 0.3391 0.3678 0.3422 0.3343 0.3430	* 213.1 * 224.0 214.2 211.3	* 0.9340 * 0.9878 0.9977 0.9732	* 24.69 * 24.95 26.09 25.24	69.23 65.53 65.14 69.95 64.66 66.90
	Elev. Temp. (250°F) (121°C)	22.84 21.27 21.68 23.08 22.22	0.3342 0.3538 0.3941 0.3373 0.3549	• • • * —	• • • * —	• • • * —	50.01 47.23 * >51.27 >49.50
Irradiated (1x10¹⁰ Rads)	Room Temp. (75°F) (24°C)	20.28 20.61 21.01 20.63	0.3906 0.3567 0.3373 0.3615	* 234.6 * 234.6	* 1.088 * 1.088	* 23.49 * 23.49	62.78 52.60 57.28 57.55
	Elev. Temp. (250°F) (121°C)	23.08 24.42 23.73 23.08 23.58	0.4037 0.4067 0.3126 0.3600 0.3708	218.8 * * 194.0 206.4	0.8850 * * * 0.8850	24.32 * * * 24.32	142.1 105.1 127.3 128.0 125.6

*Tab Slip, Data Not Available

Appendix B.

Table B.2
Individual Test Data for the Modified $[10]_4$ Laminates

Material/Temp		G_{12} (msi)	S (ksi)	$\gamma_{12_{ult}}$ (%)	E_x (msi)	σ_{ult} (ksi)	$\varepsilon_{x_{ult}}$ (%)	$\sigma_{prop\ limit}$ (ksi)
Baseline (Non-Irradiated)	Room Temp. (75°F) (24°C)	0.7914	11.06	2.540	12.49	64.67	0.6735	22.70
		0.7840	9.53	1.951	12.71	55.71	0.5288	23.51
		0.8626	9.79	1.752	12.24	57.25	0.5490	25.58
		0.7890	+	+	11.77	+	+	19.71
		0.7269	+	+	12.01	+	+	23.65
		0.8666	+	+	12.71	+	+	23.70
		0.8034	10.13	2.081	12.32	59.21	0.5837	23.14
	Elev. Temp. (250°F) (121°C)	0.6945	7.418	3.227	11.54	43.78	0.6854	15.87
		0.6017	*	*	11.03	*	*	13.13
		0.6582	6.794	2.894	11.01	41.51	0.5623	11.35
		0.5902	+	+	11.07	+	+	9.18
		0.7244	+	+	11.96	+	+	8.70
		0.7269	+	+	11.43	+	+	12.40
		0.6677	7.106	3.061	11.34	42.64	0.6239	11.77
Irradiated (1x10¹⁰ Rads)	Room Temp. (75°F) (24°C)	0.7434	9.91	*	12.76	60.36	*	22.50
		0.8010	10.08	3.467	12.14	58.96	0.8095	20.00
		0.7853	10.35	3.847	12.09	60.54	0.8139	20.14
		0.7652	+	+	12.75	+	+	22.69
		0.8332	+	+	12.76	+	+	23.46
		0.8304	+	+	12.75	+	+	25.58
		0.7931	10.12	3.657	12.54	59.95	0.8117	22.40
	Elev. Temp. (250°F) (121°C)	0.4911	*	*	8.584	*	*	4.327
		0.5277	4.392	2.972■	10.63	25.88	0.5484■	4.712
		0.4276	4.242	2.848■	8.764	31.93	0.5862■	7.019
		0.5558	+	+	10.44	+	+	7.260
		0.5101	+	+	10.73	+	+	6.346
		0.5881	+	+	10.66	+	+	9.135
		0.5167	4.317	2.910■	9.968	28.91	0.5673■	6.467

*Tab Slip, Data Not Available   + Cycled Test, Data Not Available   ■Minimum Value, Premature Gage Failure

Table B.3
Individual Test Data for the Modified [45]₄ Laminates[1]

Material/Temp		G_{12} (msi)	$\tau_{12_{ult}}$ (ksi)	$\gamma_{12_{ult}}$ (%)	E_x (msi)	$\sigma_{x_{ult}}$ (ksi)	$\varepsilon_{x_{ult}}$ (%)	$\sigma_{prop\ limit}$ (ksi)
Baseline (Non-Irradiated)	Room Temp. (75°F) (24°C)	0.6486	6.738	1.721	1.773	13.48	1.159	3.499
		0.6400	5.626	1.166	1.824	11.33	0.797	3.432
		0.7198	7.690	1.852	1.949	15.38	1.247	3.936
		0.6862	6.905	1.487	1.884	13.81	1.012	3.340
		0.7186	7.739	1.881	1.871	15.58	1.283	3.377
		0.6853	+	+	1.917	+	+	4.155
		0.6831	6.940	1.870	1.870	13.90	1.100	3.623
	Elev. Temp. (250°F) (121°C)	0.5824	4.897	2.052	1.669	10.56	1.257■	1.960
		0.5878	4.898	2.285	1.626	9.80	1.424■	2.459
		0.5490	4.956	2.066	1.563	10.31	1.280■	3.224
		0.5570	4.633	1.906	1.645	10.61	1.122■	3.128
		0.5691	4.846	2.077	1.626	10.32	1.271■	2.693
Irradiated (1×10¹⁰ Rads)	Room Temp. (75°F) (24°C)	0.7063	5.975	1.820	1.950	13.33	1.170■	2.730
		0.7118	6.214	1.567	1.882	15.03	1.095■	3.495
		0.7725	6.596	1.878	2.084	14.06	12.66■	2.485
		0.7727	+	+	2.203	+	+	2.757
		0.7956	+	+	2.178	+	+	2.929
		0.7518	6.262	1.755	2.059	14.14	1.177■	3.879
	Elev. Temp. (250°F) (121°C)	0.4836	2.652	1.268	1.496	7.064	0.7612■	1.257
		0.3916	2.299	1.195	1.223	6.760	0.7267■	1.187
		0.3917	2.153	1.112	1.215	4.305	0.6865■	1.076
		0.4223	2.368	1.192	1.311	6.043	0.7248■	1.173

■ Minimum Value, Premature Gage Failure

+ Cycled Test Data Not Available

[1] Tested at NASA LaRC

Appendix B.

84

Table B.4
Individual Test Data for the Modified [90]₄ Laminates

Material/Temp		E_2 (msi)	Y_T (ksi)	$\varepsilon_{x_{ult}}$ (%)	$\sigma_{prop\ limit}$ (ksi)
Baseline (Non-Irradiated)	Room Temp. (75°F) (24°C)	1.149 1.374 1.174 __1.233__	6.680 9.441 8.118 __8.079__	0.5905 0.7480 0.7022 __0.6802__	* 7.430 7.210 __7.320__
	Elev. Temp. (250°F) (121°C)	1.147 1.289 1.112 1.207 1.116 1.191 __1.177__	7.187 7.080 6.319 + + + __6.862__	0.6643 0.5724 0.6043 + + + __0.6136__	3.663 4.001 3.308 3.808 3.288 2.885 __3.492__
Irradiated (1x10¹⁰ Rads)	Room Temp. (75°F) (24°C)	1.777 1.452 1.314 __1.514__	6.489 * 7.197 __6.843__	0.3789 * 0.5506 __0.4424__	3.279 3.885 7.200 __4.721__
	Elev. Temp. (250°F) (121°C)	1.018 0.7916 0.7520 0.8805 0.9102 0.9294 __0.8803__	4.754 4.632 4.611 + + + __4.666__	0.4977 0.7325 0.7304 + + + __0.6535__	1.803 2.000 2.529 1.154 1.558 1.635 __1.641__

*Tab Slip, Data Not Available + Cycled Test, Data Not Available

Table B.5
Individual Test Moduli for Cycled Standard Material Laminates

Material/Temp		E_x (msi)			G_{12} (msi)	
		$[10]_4$	$[45]_4$	$[90]_4$	$[10]_4$	$[45]_4$
Baseline (Non-Irradiated)	Room Temp. (75°F) (24°C)	10.65 11.06 10.40 __10.71__	2.186 2.154 2.168 __2.169__	1.323 1.502 1.399 1.399 __1.524__ 1.430	0.7379 0.7923 0.7584 __0.7629__	0.8047 0.7970 0.7950 __0.7989__
	Elev. Temp. (250°F) (121°C)	9.220 7.919 __10.53__ 9.224	1.829 1.786 __1.830__ 1.815	1.190 __1.337__ 1.263	0.5896 0.4795 __0.6499__ 0.5730	0.6404 0.6270 __0.6403__ 0.6359
Irradiated (1x10^10 Rads)	Room Temp. (75°F) (24°C)	11.88 11.40 __11.74__ 11.68	2.644 2.499 __2.569__ 2.571	NO TESTS	0.8678 0.9464 * __0.9071__	1.010 0.9317 __0.9495__ 0.9638
	Elev. Temp. (250°F) (121°C)	8.009 7.413 __8.798__ 8.073	1.119 * __1.154__ 1.137	0.9871 0.8577 __0.9817__ 0.9422	0.3824 0.3600 __0.4906__ 0.4110	0.3848 * __0.4082__ 0.3965

*Data Not Available

BIBLIOGRAPHIC DATA SHEET	1. Report No. CCMS-86-06	2. VPI-E-86-19	3. Recipient's Accession No.

4. Title and Subtitle	5. Report Date
The Effects of Space Radiation on a Chemically Modified Graphite-Epoxy Composite Material	October 1986
	6.

7. Author(s)	8. Performing Organization Rept. No.
Susan M. Reed, George F. Sykes, Jr., Carl T. Herakovich	CCMS-86-06 VPI-E-86-19

9. Performing Organization Name and Address	10. Project/Task/Work Unit No.
Virginia Polytechnic Institute & State University Engineering Science and Mechanics Blacksburg, Virginia 24061	11. Contract/Grant No. NAG-1-343

12. Sponsoring Organization Name and Address	13. Type of Report & Period Covered
National Aeronautics and Space Administration Langley Research Center Hampton, Virginia 23665	14.

15. Supplementary Notes

16. Abstracts

The objective of this study was to characterize the effects of the space environment on the engineering properties and chemistry of a chemically modified T300/934 graphite-epoxy composite system. The material was subjected to 1.0×10^{10} rads of 1.0 MeV electron irradiation under vacuum to simulate 30 years in geosynchronous earth orbit.

Monotonic tension tests were performed at room temperature (75°F/24°C) and elevated temperature (250°F/121°C) on 4-ply unidirectional laminates. From these tests, in-plane engineering and strength properties ($E_1, E_2, \nu_{12}, G_{12}, X_T, Y_T$) were determined. Cyclic tests were also performed to characterize energy dissipation changes due to irradiation and elevated temperature.

Large diameter graphite fibers were tested to determine the effects of radiation on the stiffness and strength of graphite fibers. No significant changes were observed.

Dynamic-mechanical analysis demonstrated that the glass transition temperature was lowered by 50°F(28°C) after irradiation. Thermomechanical analysis showed the occurrence of volatile products generated upon heating of the irradiated material.

The chemical modification of the epoxy did not aid in producing a material which was more "radiation resistant" than the standard T300/934 graphite-epoxy system. Irradiation was found to cause crosslinking and chain scission in the polymer. The latter produced low molecular weight products which plasticize the material at elevated temperatures and cause apparent material stiffening at low stresses at room temperature.

17. Key Words and Document Analysis. 17a. Descriptors

composites, graphite-epoxy, tension, shear, cyclic loading, electron radiation, DMA, TMA, elevated temperature, energy dissipation

17b. Identifiers/Open-Ended Terms

17c. COSATI Field/Group

18. Availability Statement	19. Security Class (This Report) UNCLASSIFIED	21. No. of Pages 86
Distribution Unlimited	20. Security Class (This Page) UNCLASSIFIED	22. Price